PGC-1α inhibits the NLRP3 inflammasome via preserving mitochondrial viability to protect kidney fibrosis

Jong Hyun Jhee

Department of Medicine

The Graduate School, Yonsei University

PGC-1α inhibits the NLRP3 inflammasome via preserving mitochondrial viability to protect kidney fibrosis

Jong Hyun Jhee

Department of Medicine

The Graduate School, Yonsei University

PGC-1α inhibits the NLRP3 inflammasome via preserving mitochondrial viability to protect kidney fibrosis

Directed by Professor Seung Hyeok Han

The Doctoral Dissertation
submitted to the Department of Medicine,
the Graduate School of Yonsei University
in partial fulfillment of the requirements for the degree of
Doctor of Philosophy

Jong Hyun Jhee

December 2019

This certifies that the Doctoral Dissertation of Jong Hyun Jhee is approved.

Thesis Supervisor : Seung Hyeok Han

Thesis Committee Member #1 : Shin-Wook Kang

Thesis Committee Member #2 : Dong-Ryeol Ryu

Thesis Committee Member #3 : Je-Wook Yu

Thesis Committee Member #4 : Beom Jin Lim

The Graduate School
Yonsei University

December 2019

ACKNOWLEDGEMENTS

I especially wish to express my gratitude to my supervisor Professor Seung Hyeok Han, who guided me in every step of the thesis with a warm and delicate attention. I was thoughtfully taught about the extensive and in–depth review process through the logical approach to complex life science. In addition, I would like to express my deepest gratitude and appreciation to Professor Shin–Wook Kang, who is the chairman of the examination committee of my doctoral degree and eternal master, for his endless support for both education and research. I would also like to extend my gratitude to Dong–Ryeol Ryu, Je–Wook Yu, and Beom Jin Lim for their thoughtful consideration and sharp teaching. I am grateful to Professor Tae–Hyun Yoo, who gave a lot of support and encouragement to me as a good example of deep and meticulous researcher and a great educator. I would like to express my heartfelt gratitude to Professor Jung Tak Park for his devoted teaching and affection with his passion, which was endlessly lacking. I would like to express my deep gratitude to Dr. Bo Young Nam for her efforts and sacrifices. I would also like to thank Jimin Park and Dr. Seonghun Kim for their kind support during the experiments. Although I did not mention it here, I am deeply grateful to all those who have shown a lot of help and affection in the doctoral program. I think it was very extravagant luck that I could have enjoyed the opinions of professors, seniors, and colleagues who had overwhelming logic and excellent personality. I sincerely hope that the results and insights I have shown in my doctoral dissertation have contributed to the truth of the life sciences that I intend to achieve.

I would like to say that I love my parents who have shown me a resting place and unchanging faith that I can always return to. Finally, I sincerely appreciate my husband, Jae Hyun Han, who has always encouraged me with love.

Thanks everyone.

<TABLE OF CONTENTS>

LIST OF FIGURES

LIST OF TABLES

ABSTRACT

PGC-1α inhibits the NLRP3 inflammasome via preserving mitochondrial viability to protect kidney fibrosis

Jong Hyun Jhee

Department of Medicine
Yonsei University Graduate School of Medicine

(Directed by Professor Seung Hyeok Han)

Background: NOD-like receptor, pyrin domain containing protein 3 (NLRP3) contributes to inflammation, cell death, and fibrosis in kidney disease. The NLRP3 inflammasome is activated by mitochondrial damage. However, it is unknown whether peroxisomal proliferator-γ coactivator-1α (PGC-1α), a key mitochondrial biogenesis regulator, can modulate NLRP3 inflammasome pathway. Here, I demonstrated that PGC-1α inhibits activation of NLRP3 inflammasome via preserving mitochondrial viability during kidney injury.

Methods: Primary renal tubular epithelial cells (RTECs) were isolated from C57BL/6 mice. The NLRP3 inflammasome pathway, mitochondrial dynamics and morphology, oxidative stress levels, and cell injury markers were examined in RTECs treated with TGF-β1 alone, TGF-β1+PGC-1α activators (metformin and 5-aminoimidazole-4-carboxamide ribonucleotide [AICAR]) or PGC-1α plasmid, and TGF-β1+small interfering-PGC-1α. For animal study, adenine-fed mice and unilateral ureteral obstruction (UUO) mice were treated with PGC-1α activator.

Results: *In vitro*, TGF-β1 treatment to RTECs suppressed the expression levels of PGC-1α and mitochondrial dynamic-related genes. In addition, the NLRP3 inflammasome pathway was activated and the expression levels of fibrotic and apoptotic cell death markers were increased. The indirect and direct expression

of PGC-1α with the activators and the plasmid improved mitochondrial dynamics and morphology and attenuated the NLRP3 inflammasome pathway and cell injury. In contrast, these changes were accentuated by PGC-1α knock-down. The oxidative stress levels, which are inducers of the NLRP3 inflammasome after mitochondrial damage, were increased and the expression of tumor necrosis factor α-induced protein 3 (TNFAIP3), which is regulated by PGC-1α and also known as a negative regulator of NLRP3 inflammasome, was decreased by TGF-β1 and PGC-1α knock-down. However, restoration of PGC-1α significantly reversed these alterations. *In vivo*, adenine- and UUO-induced kidney injury models resulted in decreased expression levels of PGC-1α, TNFAIP3, and mitochondrial dynamics. In addition, the expression levels of oxidative stress, NLRP3 inflammasome pathway, and kidney fibrosis were increased in these mice. However, these changes were significantly reversed by treatment of PGC-1α activator.

Conclusion: This study demonstrated that kidney injury was ameliorated by PGC-1α-induced inactivation of the NLRP3 inflammasome via modulation of mitochondrial viability and dynamics.

Key words: NLRP3, PGC-1α, mitochondria, kidney fibrosis

PGC-1α inhibits the NLRP3 inflammasome via preserving mitochondrial viability to protect kidney fibrosis

Jong Hyun Jhee

Department of Medicine
Yonsei University Graduate School of Medicine

(Directed by Professor Seung Hyeok Han)

I. INTRODUCTION

Chronic kidney disease (CKD) is a global health problem and its prevalence has been rapidly increasing worldwide.[1-3] Patients with CKD have an increased risk for progression to end-stage renal disease (ESRD) and mortality.[4,5] It is therefore important to find effective therapeutic targets to prevent the progression of CKD.

Renal tubulointerstitial inflammation and fibrosis are key pathological hallmarks in progression of CKD.[6,7] These features are universal in failing kidneys and correlate strongly with renal function decline. Renal tubular epithelial cells (RTECs) account for 90% of the kidney mass and are fundamental to maintain fluid and electrolyte balance. RTECs have high baseline metabolic demands and mainly rely on adenosine triphosphate (ATP) via mitochondrial oxidative phosphorylation in energy generation.[8] Renal tubules, thus, harbor abundant mitochondria and consume a high amount of energy for reabsorption as well as excretion. Therefore, RTECs have high levels of peroxisomal proliferator-activated receptor-α (PPARα), peroxisomal proliferator-γ coactivator-1α (PGC-1α), and a dense mitochondrial network to support their metabolic and functional

needs.[9] In fact, a number of studies have suggested that mitochondrial dysfunction play a key role in kidney injury.[8]

NOD-like receptor family, pyrin domain-containing 3 (NLRP3) is involved in various host innate immune responses to microbial and nonmicrobial stimuli.[10,11] Several pathogens and endogenous danger signals released from damaged and dying cells including reactive oxygen species (ROS), extracellular ATP, monosodium urate crystals, nucleic acids, and extracellular matrix components activate the NLRP3 and lead to form a protein complex termed "inflammasome".[12] Upon activation, the NLRP3 proteins oligomerize and recruit the adaptor protein, apoptosis-associated speck-like protein containing a caspase recruitment domain (ASC), and the protease caspase-1 to form the inflammasome complex. The NLRP3 inflammasome then induces auto-process and activation of caspase-1, which results in cleavage of pro-cytokines to mature IL-1β and IL-18. Recently, the NLRP3 inflammasome has been implicated in the pathogenesis of kidney inflammation and fibrosis.[13-15] In various animal models of kidney disease, NLRP3 inflammasome pathway is activated and its final products, IL-1β and IL-18, can cause kidney tubule injury.[14-17] Conversely, blocking this pathway attenuates kidney fibrosis.[18] Interestingly, renal intrinsic cells such as TECs and podocytes express NLRP3, suggesting the potential role of NLRP3 inflammasome signaling on cellular injury.[19,20]

Growing evidence suggests that mitochondrial dysfunction, characterized by a decline in number and the depolarization, swelling, and disruption of cristae, greatly contributes to kidney fibrosis.[8] Damaged mitochondria do not efficiently produce ATP and release excessive ROS and mitochondrial DNA (mtDNA), which consequently trigger downstream inflammatory responses and lead to cell death and tubular injury. Moreover, recent studies have demonstrated the potential interaction between mitochondrial dysfunction and NLRP3 inflammasome activation in renal tubular injury models.[21-23] However, it is unknown whether PGC-1α, a key mitochondrial biogenesis regulator, can

regulate NLRP3 pathway via modulating mitochondrial dynamics.

Thus, I investigated the role of PGC-1α in the regulation of the NLRP3 inflammasome activation in RTECs. In particular, I examined whether altered mitochondrial viability and dynamics induced by activation or suppression of PGC-1α can regulate NLRP3 inflammasome pathway, and thus affect kidney injury.

II. MATERIALS AND METHODS

1. Primary cell cultures

RTECs were isolated from C57BL/6 mice. The cells were cultured in the Dulbecco's Modified Eagle Medium (DMEM) (Gibco, Thermo Fisher Scientific, Waltham, MA, USA) containing 10% fetal bovine serum (FBS) (Gibco, Thermo Fisher Scientific, Waltham, MA, USA), 100 U/ml penicillin G (Sigma-Aldrich, UK), 2.5 mg/ml amphotericin B (Sigma-Aldrich, UK), and 20 ng/ml epidermal growth factor (EGF) (Sigma-Aldrich, UK). In short, kidneys were dissected, placed in 1 ml ice-cold Dulbecco's Phosphate-Buffered Saline (DPBS) (Gibco, Thermo Fisher Scientific, Waltham, MA, USA), and minced into pieces of approximately 1 mm^3. These pieces were transferred and digested for 60 minutes at 37℃, and the supernatants were sieved through a 100-mm nylon mesh. After centrifugation for 10 minutes at 3000 rpm, the pellet was resuspended in sterile red blood cell lysis buffer (8.26 g NH_4Cl, 1 g $KHCO_3$, and 0.037 g EDTA per 1 L double distilled H_2O) and seeded in 10 cm culture dishes.

2. Treatment of TGF-β1 and PGC-1α activators, and transfections to primary RTECs

Subconfluent RTECs were FBS-restricted for 24 hours, and then the medium was replaced with 1% FBS DMEM medium for the control group and the same medium with TGF-β1 (5 ng/ml) (R&D systems, Minneapolis, MN, USA) for the

TGF-β1 group. RTECs were harvested for RNA and protein analyses at 48 hours after media changes. PGC-1α activators, metformin (10 mM) and 5-aminoimidazole-4-carboxamide ribonucleotide (AICAR, 1 mM), were treated for both control and TGF-β1 groups. Both groups were also transfected with PGC-1α plasmid (1 μg) (Addgene, Cambridge, MA, USA) and PGC-1α small interfering RNA (siRNA), using Lipofectamine 2000 and Plus reagents (Invitrogen, Carlsbad, CA, USA). Next, 6 hours after transfection, media were changed to serum-free media, and the cells were incubated for an additional 48 hours.

3. Animal study and treatment

Male C57BL/6 mice (6 weeks old, initial weight 20 g) were purchased from The Jackson Laboratory (Bar Harbor, ME, USA). The animals were maintained in a temperature–controlled room (22°C) in a 12 hours light/dark cycle. One week after arrival, animals were divided into two groups and fed with either normal diet (ND; $n = 10$) or 0.2% adenine diet (AD; $n = 10$) for up to 4 weeks. Both ND and AD groups were also daily treated with intraperitoneal injection of PGC-1α activating drug, metformin (250 mg/kg), at one week before diet start. After 4 weeks of ND or AD, animals were sacrificed and the kidneys were extracted while anesthetized with Zoletil (10 mg/kg) (Virbac, Carros, France). Unilateral ureter obstruction (UUO) was performed as described previously.[24] In short, mice were anesthetized with Zoletil (10 mg/kg) (Virbac, Carros, France) and the left ureter was exposed via an incision under 0.5 cm from costal margin. The mid-ureter was then obstructed using a ligation with silk sutures. The sham-operated mice underwent the same procedure without the obstruction of the ureter and used as controls. Both sham and UUO mice were daily treated with intraperitoneal injection of metformin (250 mg/kg) and AICAR (500 mg/kg). Mice were sacrificed at 5 days after UUO and the kidneys were removed while anesthetized.

Kidney samples were then immediately frozen in liquid nitrogen and stored at -

80°C until use. The protocols for animal experiments were approved by the Committee for the Care and Use of Laboratory Animals at Yonsei University College of Medicine in Seoul, Republic of Korea (No. H14C2003). All experiments with animals were conducted in accordance with the Principles of Laboratory Animal Care (NIH Publication no. 85–23, revised 1985).

4. Total RNA extraction

Whole kidney samples were rapidly frozen using liquid nitrogen and homogenized by mortar and pestle thrice with 700 μl of RNAiso reagent (Takara Bio Inc., Otsu, Shiga, Japan). For RTECs, 700 μl of RNAiso were added to the cell culture dish, and the suspension was collected and homogenized for 5 minutes at room temperature (RT). After then, 160 μl of chloroform was added into the homogenized samples of the kidneys and cells. Next, the mixture was shaken vigorously for 30 seconds, stored for 3 minutes at RT, and centrifuged 12,000 rpm for 15 minutes at 4℃. The aqueous phase located in the top of three phases was transferred to a fresh tube carefully not to be contaminated with the other phases. Extracted RNA was precipitated by adding 400 μl of isopropanol, and centrifuged at 12,000 rpm for 30 minutes at 4℃. The RNA pellet was washed with 70% ethanol, air-dried for 2 minutes, and dissolved in sterile diethyl pyrocarbonate (DEPC)-treated distilled water. The quantity and quality of extracted RNA were assessed by spectrophotometric measurements at wavelengths of 260 and 280 nm.

5. Reverse transcription

A Takara cDNA synthesis kit (Takara Bio Inc., Otsu, Shiga, Japan) was used to obtain first strand cDNA. Reverse transcription was conducted using 2 μg of total RNA extracts with 10 μM random hexanucleotide primer, 1 mM dNTP, 8 mM $MgCl_2$, 30 mM KCl, 50 mM Tris-HCl at pH 8.5, 0.2 mM dithiothreithol, 25 U RNase inhibitor, and 40 U PrimeScript reverse transcriptase. The mixture was incubated for 10 minutes at 30℃, and for 1 hour at 42℃, followed by incubation

for 5 minutes at 99℃ for the inactivation of the enzyme.

6. Real–time quantitative polymerase chain reaction

The RNAs used for amplification were 25 ng per reaction tube. Using the ABI PRISM 7700 Sequence Detection System (Applied Biosystems, Foster City, CA, USA), a total volume of 20 μl mixture in each well was used containing 10 μl of SYBR Green PCR Master Mix (Applied Biosystems, Foster City, CA, USA), 5 μl of cDNA, and 5 pmol sense and antisense primers. The primer concentrations were determined by preliminary experiments that analyzed the optimal concentrations of each primer. The quantitative polymerase chain reaction (qPCR) conditions were as follows: 35 cycles of denaturation for 30 minutes at 94.5℃, annealing for 30 seconds at 60℃, and extension for 1 minute at 72℃. Initial heating for 9 minutes at 95℃ and final extension for 7 minutes at 72℃ were performed for all PCR reactions. The primer sequences used in this study were described in **Table 1**. Each sample was run in triplicate in separated tubes and a control without cDNA was also run in parallel with each assay. After real-time PCR, the temperature was increased from 60 to 95℃ at a rate of 2℃/minute to construct a melting curve. The cDNA content of each specimen was determined using a comparative C_T method with $2^{-\Delta\Delta CT}$. The results were given as the relative expression normalized to the expression of 18s ribosomal RNA (rRNA) and expressed in arbitrary units.

Table 1. Sequences of oligonucleotide primers used for qPCR test

Genes		Sequences
Ppargc1α	**Forward**	AGTCCCATACACAACCGCAG
	Reverse	CCCTTGGGGTCATTTGGTGA
Mfn	**Forward**	TTGGAAAACAGTGGGCTGGA
	Reverse	AACGCTCTCTCTTTCGCACG
Drp1	**Forward**	GCTGCCTCAGATCGTCGTAG
	Reverse	GGTGACCACACCAGTTCCTC
Tfam	**Forward**	GGAATGTGGAGCGTGCTAAAA
	Reverse	TGCTGGAAAAACACTTCGGAATA

mtDNA	**Forward**	TTTTATCTGCATCTGAGTTT
	Reverse	CCACTTCATCTTACCATTTA
16s	**Forward**	AGTAAGAACAAGCAAAGAT
	Reverse	TCGTTTGGTTTCGGGGTTTC
Nlrp3	**Forward**	CTCCGGTTGGTGCTTAGACT
	Reverse	TCCCAGACACTCATGTTGGC
ASC	**Forward**	GCACAGGCAAGCACTCATTG
	Reverse	ACGAACTGCCTGGTACTGTC
IL-1β	**Forward**	ATCTCGCAGCAGCACATCAA
	Reverse	AAGGTCCACGGGAAAGACAC
IL-18	**Forward**	CGGCCAAAGTTGTCTGATTCC
	Reverse	ACTCTTGCGTCAACTTCAAGG
FN	**Forward**	TGACAACTGCCGTAGACCTGG
	Reverse	TACTGGTTGTAGGTGTGGCCG
Col1	**Forward**	GAGCGGAGAGTACTGGATCG
	Reverse	GCTTCTTTTCCTTGGGGTTC
Bcl–2	**Forward**	AGGAGCAGGTGCCTACAAGA
	Reverse	GCATTTTCCCACCACTGTCT
Bax	**Forward**	TCCACCAAGAAGCTGAGCGAG
	Reverse	GTCCAGCCCATGATGGTTCT
18s	**Forward**	CGCTTCCTTACCTGGTTGAT
	Reverse	GGCCGTGCGTACTTAGACAT

7. Western blot analyses

Protein expression levels of the NLRP3 inflammasome pathway, oxidative stress marker, and profibrotic markers were examined with Western blot analyses. Harvested cultured cells and the mouse kidneys were lysed in sodium dodecyl sulfate (SDS) sample buffer [2% SDS, 10 mM Tris-HCl, pH 6.8, 10% (vol/vol) glycerol]. Lysate was centrifuged at 10,000 g for 10 minutes at 4℃, and the supernatant was stored at -70℃. Protein concentrations were determined with a Bio-Rad kit (Bio-Rad Laboratories, Inc., Hercules, CA, USA). Laemmli sample buffer was added to aliquots of 50 μg of the protein extracts, which were heated for 5 minutes at 100℃ and electrophoresed in acrylamide denaturating SDS-polyacrylamide gel. A Hybond-ECL membrane was used to transfer protein using a Hoeffer semidry blotting apparatus (Hoeffer Instruments, San Francisco, CA, USA). After the protein was transferred to the membrane, it was incubated in

blocking buffer A (PBS, 0.1% Tween-20, and 5% nonfat milk) for 1 hour at RT, and then incubated overnight at 4℃ in a 1:1,000 dilution of following polyclonal antibodies; PGC-1α (Abcam, Cambridge, MA, USA), NLRP3 (Adipogen Life Sciences, CA, USA), ASC (Cell Signaling Technology, MA, USA), IL-1β (Abcam, Cambridge, MA, USA), IL-18 (Abcam, Cambridge, MA, USA), tumor necrosis factor α induced protein 3, (TNFAIP3) (Cell Signaling Technology, MA, USA), fibronectin (DAKO, Carpentaria, CA, USA), type I collagen (Southern Biotech, Birmingham, AL, USA), Bax (Santa Cruz Biotechnology, Santa Cruz, CA, USA), B cell lymphoma–2 (Bcl–2) (Santa Cruz Biotechnology, Santa Cruz, CA, USA), Caspase-3 (Cell Signaling Technology, MA, USA), and β–actin (Sigma–Aldrich, UK). A horseradish peroxidase (HRP)–conjugated anti–rabbit (Santa Cruz Biotechnology, Santa Cruz, CA, USA) or anti–mouse IgG antibody (Santa Cruz Biotechnology, Santa Cruz, CA, USA) were used as secondary antibodies. After frequent rinses, the membranes were developed by chemiluminescence (Gibco, Thermo Fisher Scientific, Waltham, MA, USA). To quantify the band densities, Image J software (National Institutes of Health, Bethesda, MD; online at http://rsbweb.nih.gov/ij) was used. The changes in the optical densities of bands from the treated groups relative to control cells or tissues were used for analysis.

8. Assay of NLRP3 inflammasome assembly

To determine the oligomerization of ASC, a disuccinimidyl suberate (DSS) (Gibco, Thermo Fisher Scientific, Waltham, MA, USA)-mediated cross-linking assay was performed as described previously.[25] In brief, kidney tissue samples were mixed in 1 ml of OPTI-MEM I medium for 2 hours in the absence or presence of AD. The samples were pelleted by centrifugation and lysed in 0.5 ml of ice-cold buffer A. The lysates were centrifuged at 6000 rpm at 4℃ for 10 minutes. The pellets were washed twice with PBS and then resuspended in 500 μl PBS. The re-suspended pellets were cross-linked with fresh DSS (2 mM) for

30 minutes, and then pelleted by centrifugation at 6000 rpm for 10 minutes. The cross-linked pellets were resuspended in 30 μl SDS sample buffer and fractionated on 12% SDS polyacrylamide gel followed by immunoblotting with ASC antibody (Cell Signaling Technology, MA, USA).

9. Measurement of oxidative stress levels

Oxidative stress (malondialdehyde [MDA]) levels were measured in RTECs and kidney tissues using an MDA assay kit (Abcam, Cambridge, MA, USA). Ten mg of RTECs were homogenized on ice in 300 μl of MDA lysis buffer (Abcam, Cambridge, MA, USA), then centrifuged (13,000×g, 10 minutes) to remove insoluble materials. Ten ml of plasma were mixed with 500 μl of 42 mM H_2SO_4 and 125 μl of phosphotungstic acid solution at RT for 5 minutes. After centrifuging (13,000×g, 3 minutes), the pellet was re-suspended on ice with 100 μl of double-distilled H_2O. Then, 200 μl of solution and 600 μl of 2-thiobarbituric acid solution were incubated at 95℃ for 60 minutes before cooling to RT in the ice bath for 10 minutes. The intensity of absorbance at 532 nm was proportional to the MDA level. To measure mitochondrial ROS production, cells were resuspended in Hank's Balanced Salt Solution after appropriate treatments, and stained with MitoSOX (Gibco, Thermo Fisher Scientific, Waltham, MA, USA) at 37℃ for 20 minutes.

10. Isolation of mitochondria

RTECs were fractionated into cytosol and mitochondria by using Mitochondria isolation kit (BioVision, Inc. CA, USA) as per the manufacturer's protocol.[26] In short, cells were collected and washed with 10 ml ice cold PBS. Cells were centrifuged at 600×g for 5 minutes at 4℃ and resuspended in 1.0 ml of 1X Cytosol Extraction Buffer. Homogenization was performed on ice and centrifuged at 1,200×g for 10 minutes at 4℃ to remove nuclei and intact cells. The collected supernatant was centrifuged at 10,000×g for 30 minutes at 4℃. The

resulting pellets were resuspended in 1.0 ml of 1X Cytosol Extraction Buffer and centrifuged at 10,000×g for 30 minutes at 4℃ to obtain mitochondria. The obtained mitochondria were lysed in 30 μl of Mitochondrial Lysis Buffer and added to 100ul Enzyme B Mix with 100 μl absolute ethanol. After centrifugation, resulting pellet was mtDNA. The cytosolic mtDNA was obtained from the supernatant after precipitation with ethanol. The concentration of mtDNA was determined by qPCR assay.

11. Electron microscopic examination

I next examined mitochondrial structure by standard transmission electron microscopy. Primary RTECs were fixed with a mixture of 2% paraformaldehyde and 2.5% glutaraldehyde overnight, washed, dehydrated, and embedded in a resin according to standard procedures. Mitochondria were examined under a JEOL 1011 microscope (JEOL, Tokyo, Japan).

12. Histological and Immunofluorescent staining

To evaluate histologic features, formalin-fixed, paraffin-embedded kidney sections were stained with Masson's trichrome reagent. All slide pictures were captured using an Olympus DP73 microscope.

For immunofluorescent staining for mitochondria, MitoTracker Deep Red (Gibco, Thermo Fisher Scientific, Waltham, MA, USA) was used. RTECs were fixed in 4% paraformaldehyde and blocked in DPBS containing 5% normal rabbit serum and 0.1% Tween-20. Cells were then stained with anti-mouse NLRP3, MitoTracker, followed by AlexaFluor594-conjugated goat anti-rabbit antibodies (Jackson ImmunoResearch, West Grove, PA), and finally slides were mounted with DAPI and imaged.

13. Enzyme-linked immunosorbent assay

Levels of IL-1β and IL-18 in RTECs and the kidney tissues were determined

using commercial enzyme-linked immunosorbent assay (ELISA) kits (R&D Systems, Minneapolis, MN, USA).

14. Statistical analyses

Statistical analyses were performed using IBM SPSS software for Windows version 23.0 (IBM Corporation, Armonk, NY, USA). Continuous variables are presented as mean ± standard deviation, and categorical variables are shown as numbers (percentage). To analyze differences between two groups, Mann–Whitney U test was used, and Kruskal–Wallis test was applied for comparison between more than two groups. For all analyses, $P < 0.05$ was considered statistically significant.

III. RESULTS

1. The alterations in PGC-1α, mitochondrial dynamics, and NLRP3 inflammasome pathway in TGF-β1-treated RTECs

First, I examined the expression of PGC-1α, mitochondrial dynamics, and NLRP3 pathway in RTECs treated with TGF-β1. In these cells, TGF-β1 treatment decreased the transcript and protein levels of PGC-1α (**Fig. 1A and B**). Accordingly, mRNA expression levels of mitofusin (*Mfn*), a mitochondrial fusion-related gene, and mitochondrial transcription factor A (*Tfam*), which represents mitochondrial mass, were significantly decreased, whereas that of dynamin-related protein 1 (*Drp1*), a mitochondrial fission-related gene, was increased compared with control (**Fig. 1C-E**). In addition, TGF-β1 treatment activated NLRP3 inflammasome signaling evidenced by increased expression levels of NLRP3 inflammasome pathway-related genes and proteins (**Fig. 2A-E**). Furthermore, expression levels of fibrotic markers including fibronectin and collagen 1, and apoptotic cell death index of Bax/bcl-2 ratio and cleaved-caspase 3 were also increased (**Fig. 2F-I**).

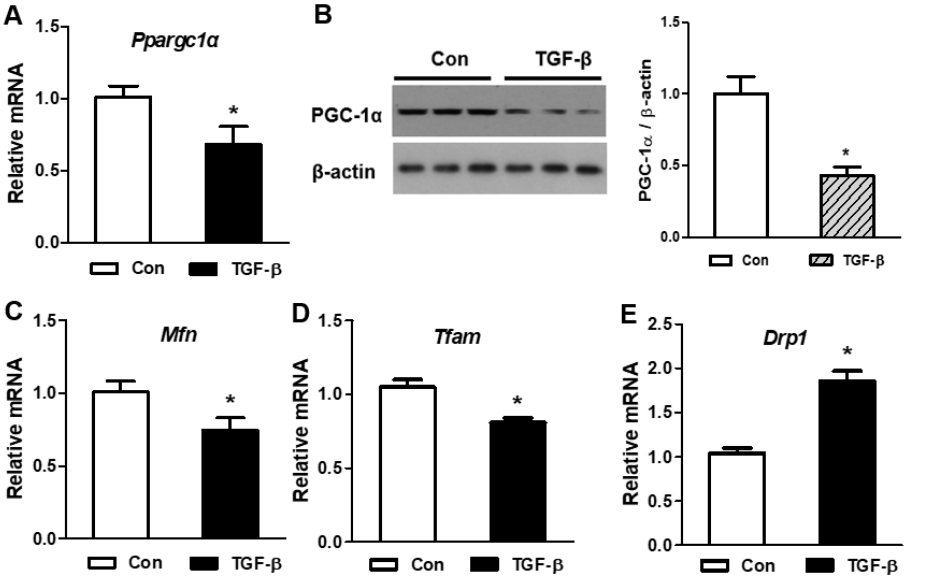

Figure 1. Changes in PGC-1α expression and mitochondrial dynamics in TGF-β1-treated RTECs. (A) mRNA and **(B)** protein expression levels of PGC-1α were decreased in TGF-β1-treated RTECs. **(C-E)** mRNA expression of mitochondrial dynamic-related genes including *Mfn*, *Tfam*, and *Drp1*were altered in TGF-β1-treated RTECs.

Note: * $P<0.05$ vs. control.

Abbreviations: PGC-1α, peroxisomal proliferator-γ coactivator-1α; RTEC, renal tubular epithelial cell; Mfn, mitofusin; Tfam, mitochondrial transcriptional factor A; Drp1, dynamin related protein 1.

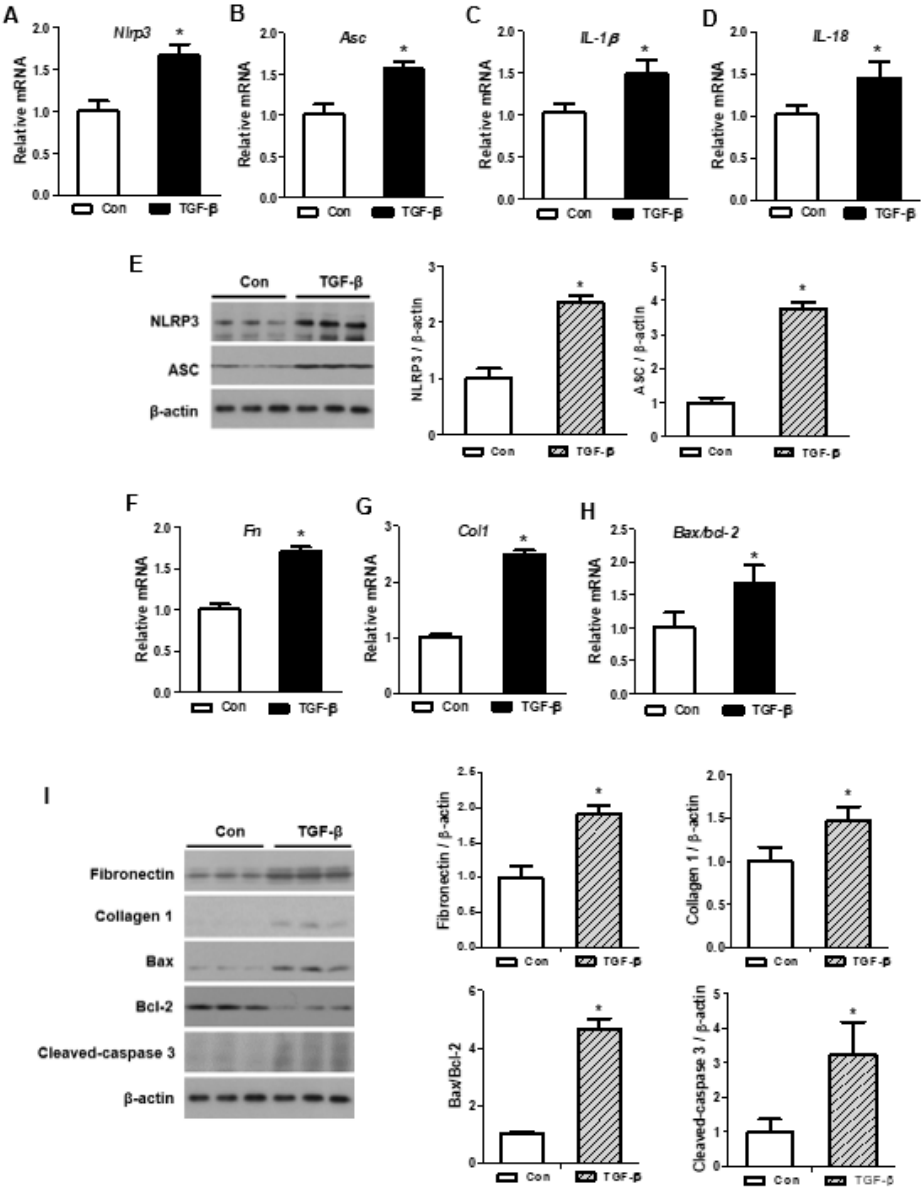

Figure 2. Changes in NLRP3 inflammasome pathway and cell injury in TGF-β1-treated RTECs. (A-D) mRNA and **(E)** protein expression levels of NLRP3 inflammasome pathway were increased in TGF-β1-treated RTECs. **(F-H)** mRNA and **(I)** protein expression levels of fibrotic markers including fibronectin and collagen 1, and apoptotic cell death markers of Bax/bcl-2 and

cleaved caspase-3 were increased in TGF-β1-treated RTECs.

Note: * $P<0.05$ vs. control.

Abbreviations: PGC-1α, peroxisomal proliferator-γ coactivator-1α; NLRP3, NOD-like receptor family, pyrin domain-containing 3; RTEC, renal tubular epithelial cell.

2. PGC-1α restores mitochondrial dynamics and morphology and attenuates the NLRP3 inflammasome activation and cell injury

PGC-1α is a key regulator of mitochondria biogenesis. Thus, I then evaluated whether PGC-1α could attenuate cell injury by suppressing NLRP3 inflammation pathway. To this end, I first used indirect activators of PGC-1α including metformin and AICAR. These PGC-1α activators restored the altered expression of PGC-1α (**Fig. 3A and B**) and mitochondrial dynamic-related genes and mitochondrial mass caused by TGF-β1 in RTECs (**Fig. 3C-E**). Moreover, the increased expression levels of NLRP3 inflammasome pathway (**Fig. 4A-F**), fibrotic markers, and apoptotic cell death index in TGF-β1-treated cells were concomitantly decreased by PGC-1α activators (**Fig. 4G-J**). Accordingly, additional experiments with direct overexpression using PGC-1α plasmid restored the decreased expression of PGC-1α and mitochondrial dynamic-related genes and mitochondrial mass caused by TGF-β1 in RTECs **(Fig. 5A-B)**. The increased expression levels of NLRP3 inflammasome pathway, fibrotic markers, and apoptotic cell death index in TGF-β1-treated cells were attenuated by direct overexpression of PGC-1α **(Fig. 6A-J)**. These findings were corroborated by additional experiments with direct overexpression using PGC-1α plasmid (**Fig. 5A-D and Fig. 6A-J**). To substantiate these findings, I further examined mitochondrial morphological changes by MitoTracker Red staining (**Fig. 7A**). TGF-β1 decreased the staining intensity of MitoTracker and these were restored by PGC-1α overexpression. Conversely, the increased expression of NLRP3 in TGF-β1-treated RTECs was reduced by PGC-1α overexpression. The mtDNA copy numbers were decreased in mitochondrial fraction and increased in cytosolic fraction after TGF-β1 treatment, suggesting that mtDNA was released from mitochondria into cytosol. However, these changes were restored after direct overexpression of PGC-1α (**Figure 7B**).

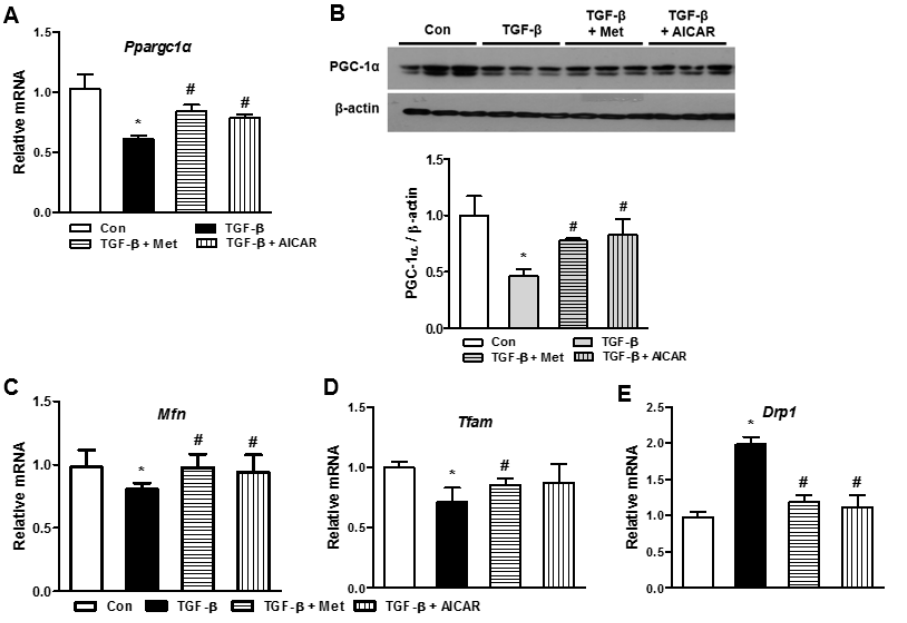

Figure 3. PGC-1α activators restore mitochondrial dynamics and morphology in TGF-β1-treated RTECs. (A) mRNA and **(B)** protein expression levels of PGC-1α were restored in TGF-β1-treated RTECs with PGC-1α activators. **(C-E)** mRNA expression levels of mitochondrial dynamic-related genes were restored in TGF-β1-treated RTECs with PGC-1α activators.

Note: * P<0.05 vs. control; # P<0.05 vs. TGF-β1-treated RTECs.

Abbreviations: PGC-1α, peroxisomal proliferator-γ coactivator-1α; RTEC, renal tubular epithelial cell; Met, metformin; AICAR, 5-aminoimidazole-4-carboxamide ribonucleotide; Mfn, mitofusin; Tfam, mitochondrial transcriptional factor A; Drp1, dynamin related protein 1.

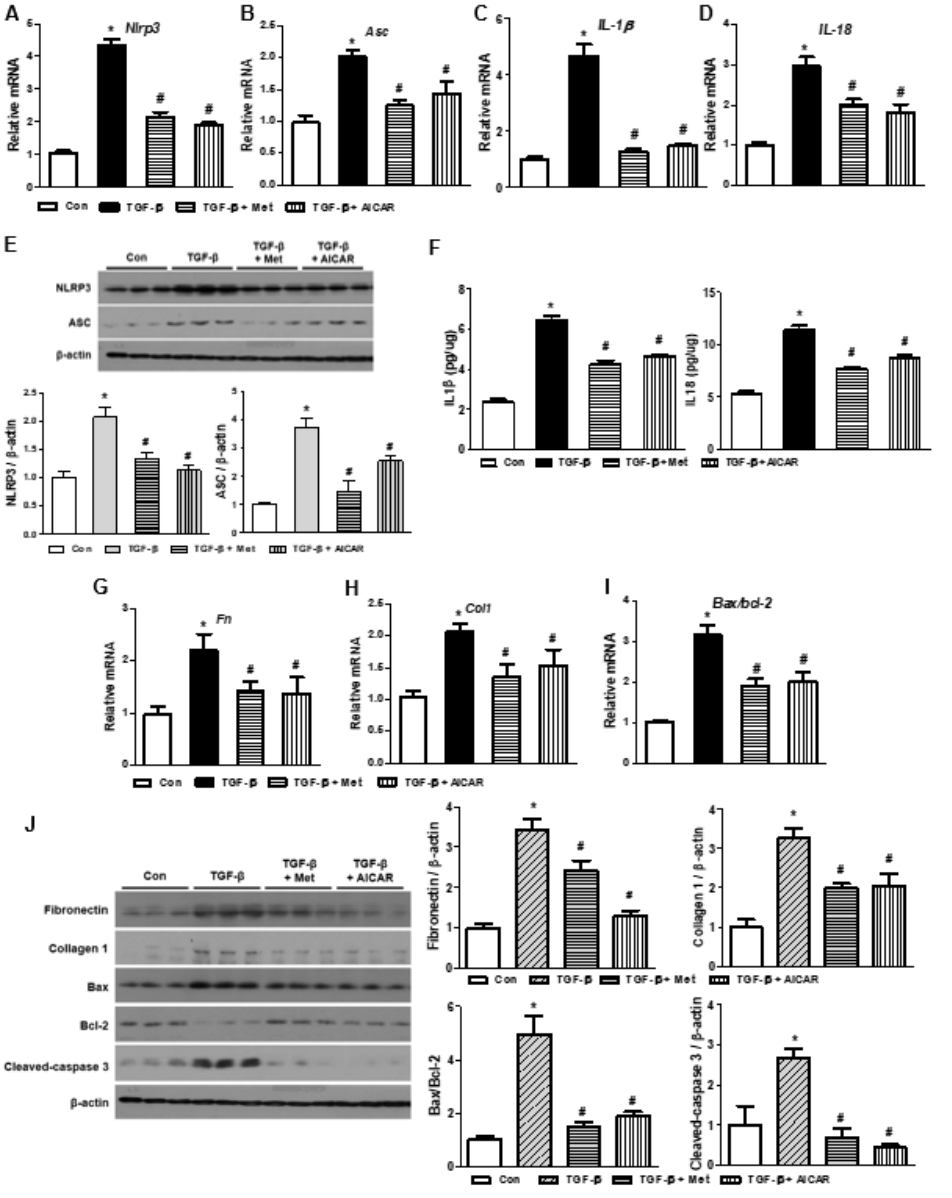

Figure 4. PGC-1α activators attenuate the NLRP3 inflammasome activation and cell injury. (A-D) mRNA and **(E)** protein expression levels of NLRP3 inflammasome pathway and **(F)** concentrations of IL-1β and IL-18 assessed by ELISA were reduced in TGF-β1-treated RTECs with PGC-1α activators. **(G-I)** mRNA and **(J)** protein expression levels of fibrotic and apoptotic markers were

attenuated in TGF-β1-treated RTECs with PGC-1α activators.

Note: * $P<0.05$ vs. control; # $P<0.05$ vs. TGF-β1-treated RTECs.

Abbreviations: PGC-1α, peroxisomal proliferator-γ coactivator-1α; NLRP3, NOD-like receptor family, pyrin domain-containing 3; ELISA, enzyme-linked immunosorbent assay; RTEC, renal tubular epithelial cell; Met, metformin; AICAR, 5-aminoimidazole-4-carboxamide ribonucleotide.

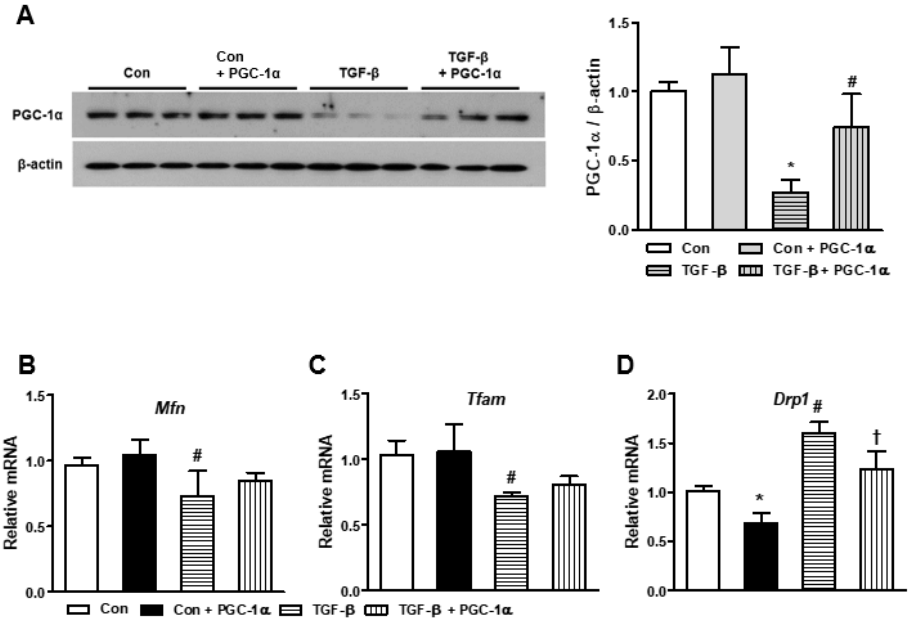

Figure 5. Direct overexpression of PGC-1α restores mitochondrial dynamics and morphology. (A) protein expression level of PGC-1α was restored in TGF-β1-treated RTECs after transfection of PGC-1α plasmid. **(B-D)** mRNA expression levels of mitochondrial dynamic-related genes in TGF-β1-treated RTECs revealed trends of restoration after transfection of PGC-1α plasmid.

Note: *, # $P<0.05$ vs. control; † $P<0.05$ vs. TGF-β1-treated RTECs.

Abbreviations: PGC-1α, peroxisomal proliferator-γ coactivator-1α; RTEC, renal tubular epithelial cell; Mfn, mitofusin; Tfam, mitochondrial transcriptional factor A; Drp1, dynamin related protein 1.

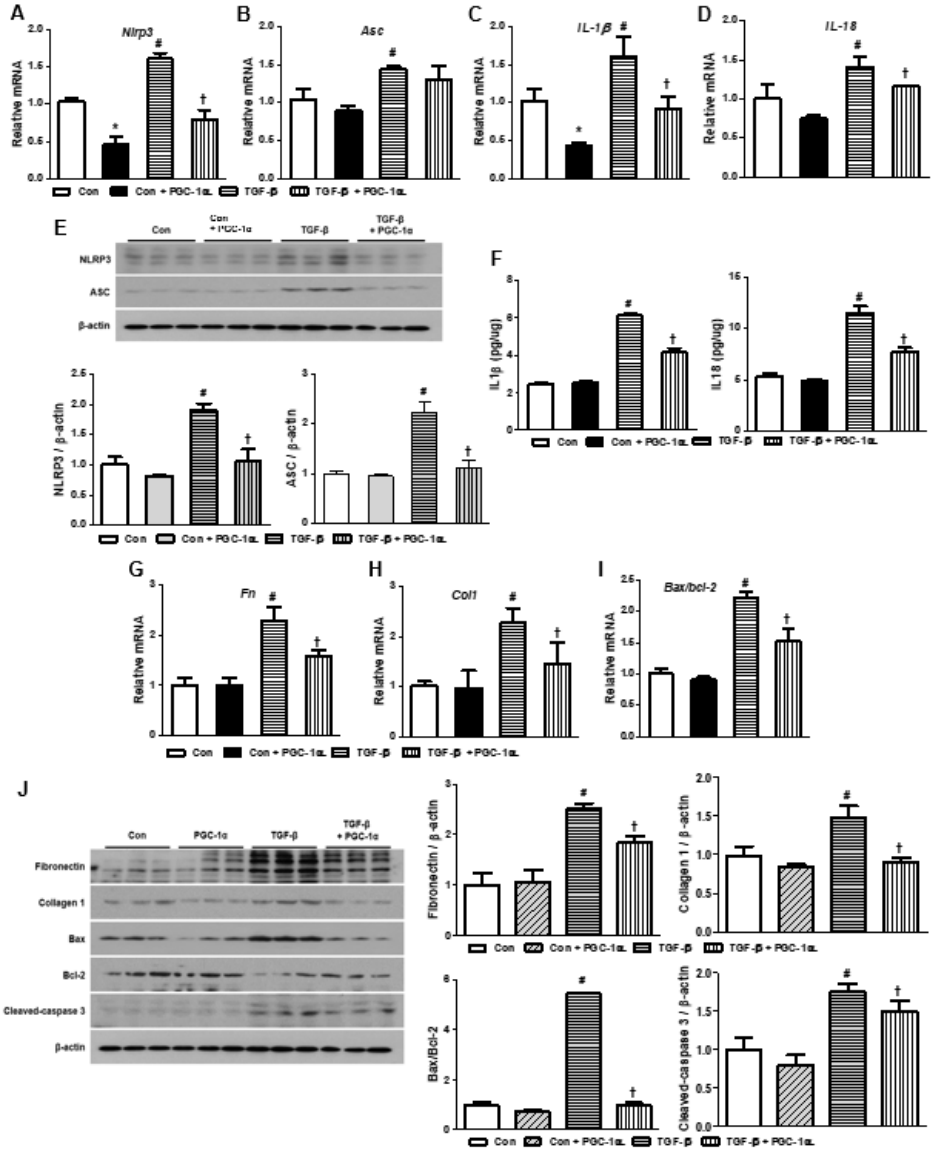

Figure 6. Direct overexpression of PGC-1α attenuates the NLRP3 inflammasome activation and cell injury. (A-D) mRNA and **(E)** protein expression levels of NLRP3 inflammasome pathway and **(F)** concentrations of IL-1β and IL-18 assessed by ELISA were reduced in TGF-β1-treated RTECs with transfection of PGC-1α plasmid. **(G-I)** mRNA and **(J)** protein expression levels of fibrotic and apoptotic markers were attenuated in TGF-β1-treated RTECs with

transfection of PGC-1α plasmid.

Note: *, # $P<0.05$ vs. control; † $P<0.05$ vs. TGF-β1-treated RTECs.

Abbreviations: PGC-1α, peroxisomal proliferator-γ coactivator-1α; NLRP3, NOD-like receptor family, pyrin domain-containing 3; ELISA, enzyme-linked immunosorbent assay; RTEC, renal tubular epithelial cell.

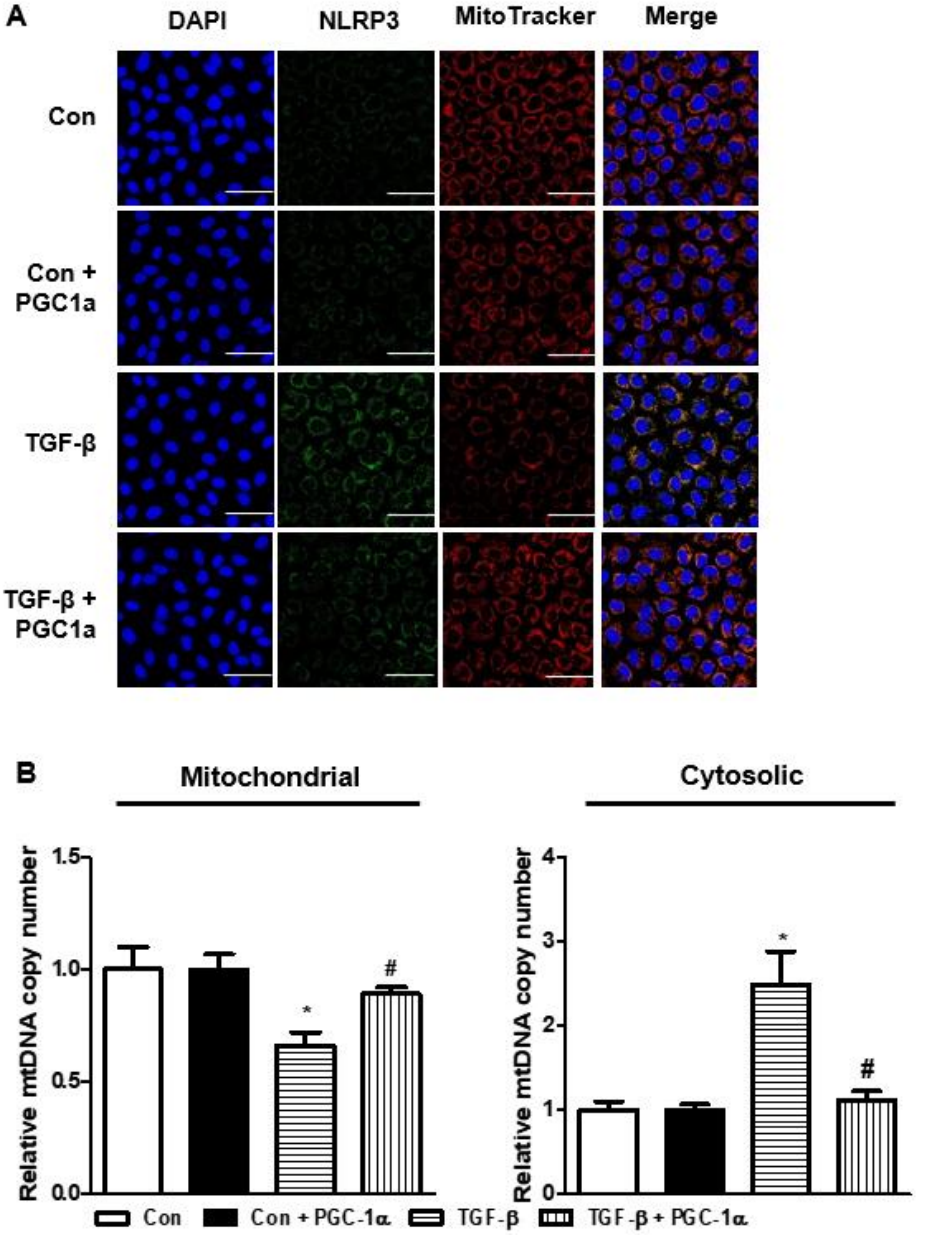

Figure 7. Localization of NLRP3 with mitochondria and assessment of mtDNA counts in TGF-β1-treated RTECs with or without PGC-1α overexpression. (A) Confocal microscopy with Immunofluorescent staining revealed co-localization of NLRP3 (green) with the destructed mitochondria (red)

in TGF-β1-treated RTECs, which were restored by PGC-1α overexpression. The blue signal represents nuclear fluorescence. **(B)** MtDNA copy numbers were decreased in mitochondrial fraction, while increased in cytosolic fraction in TGF-β1-treated RTECs, which were reversed by PGC-1α overexpression.

Note: * $P<0.05$ vs. control; # $P<0.05$ vs. TGF-β1-treated RTECs.

Abbreviations: NLRP3, NOD-like receptor family, pyrin domain-containing 3; mtDNA, mitochondrial DNA; RTEC, renal tubular epithelial cell; PGC-1α, peroxisomal proliferator-γ coactivator-1α.

3. PGC-1α deficiency results in activation of NLRP3 inflammasome and worsens cell injury

To further clarify the mechanistic link between PGC-1α and NLRP3 inflammasome pathway, I conversely knocked down PGC-1α gene. PGC-1α gene was effectively silenced by siRNA against *Ppargc1α* (siPGC-1α) (**Fig. 8A and B**). PGC-1α deficiency decreased the expression of *Mfn* and *Tfam*, but increased the expression of *Drp1* (**Fig. 8C-E**). These changes were further exacerbated in TGF-β1-treated cells with PGC-1α knock-down. In accordance with these, the expression of NLRP3, IL-1β, and IL-18 were more increased in these dual treatment cells (**Fig. 9A-E**). The concentrations of IL-1β and IL-18 were further elevated after treatment of siPGC-1α measured by ELISA (**Fig. 9F**). Furthermore, PGC-1α knock-down together with TGF-β1 worsened cell injury evidenced by more increased expression of profibrotic and apoptotic markers (**Fig. 9G-J**).

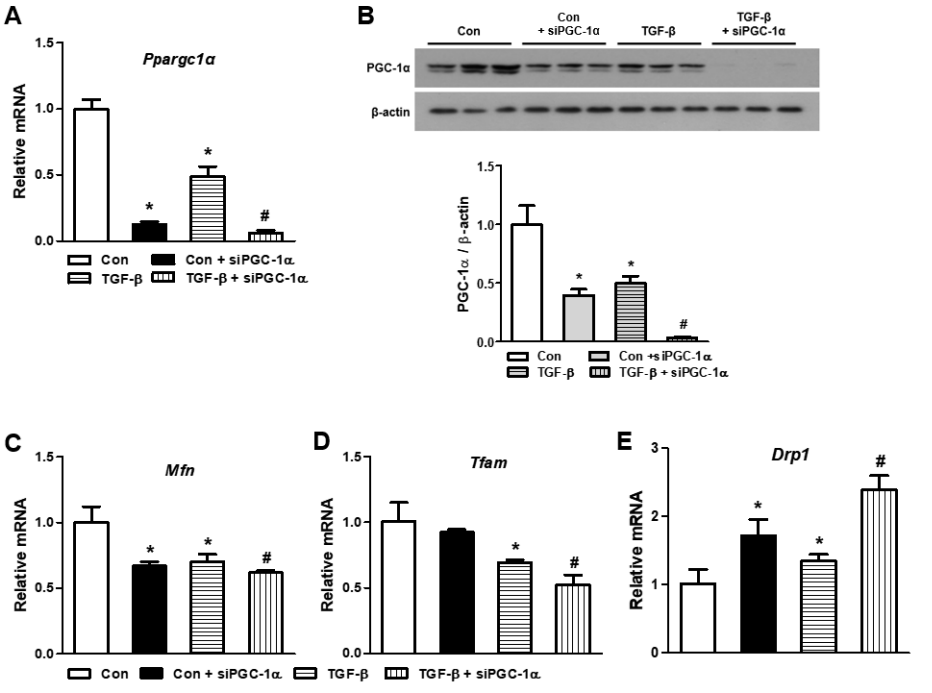

Figure 8. Downregulation of PGC-1α gene increases mitochondrial damage. **(A)** mRNA and **(B)** protein expression levels of PGC-1α were downregulated in TGF-β1-treated RTECs with siPGC-1α. **(C-E)** mRNA expression levels of mitochondrial dynamic-related genes were dysregulated in TGF-β1-treated RTECs with siPGC-1α.

Note: * $P<0.05$ vs. control; # $P<0.05$ vs. TGF-β1-treated RTEC.

Abbreviations: PGC-1α, peroxisomal proliferator-γ coactivator-1α; RTEC, renal tubular epithelial cell; Met, metformin; siRNA, small interfering RNA; Mfn, mitofusin; Tfam, mitochondrial transcriptional factor A; Drp1, dynamin related protein 1.

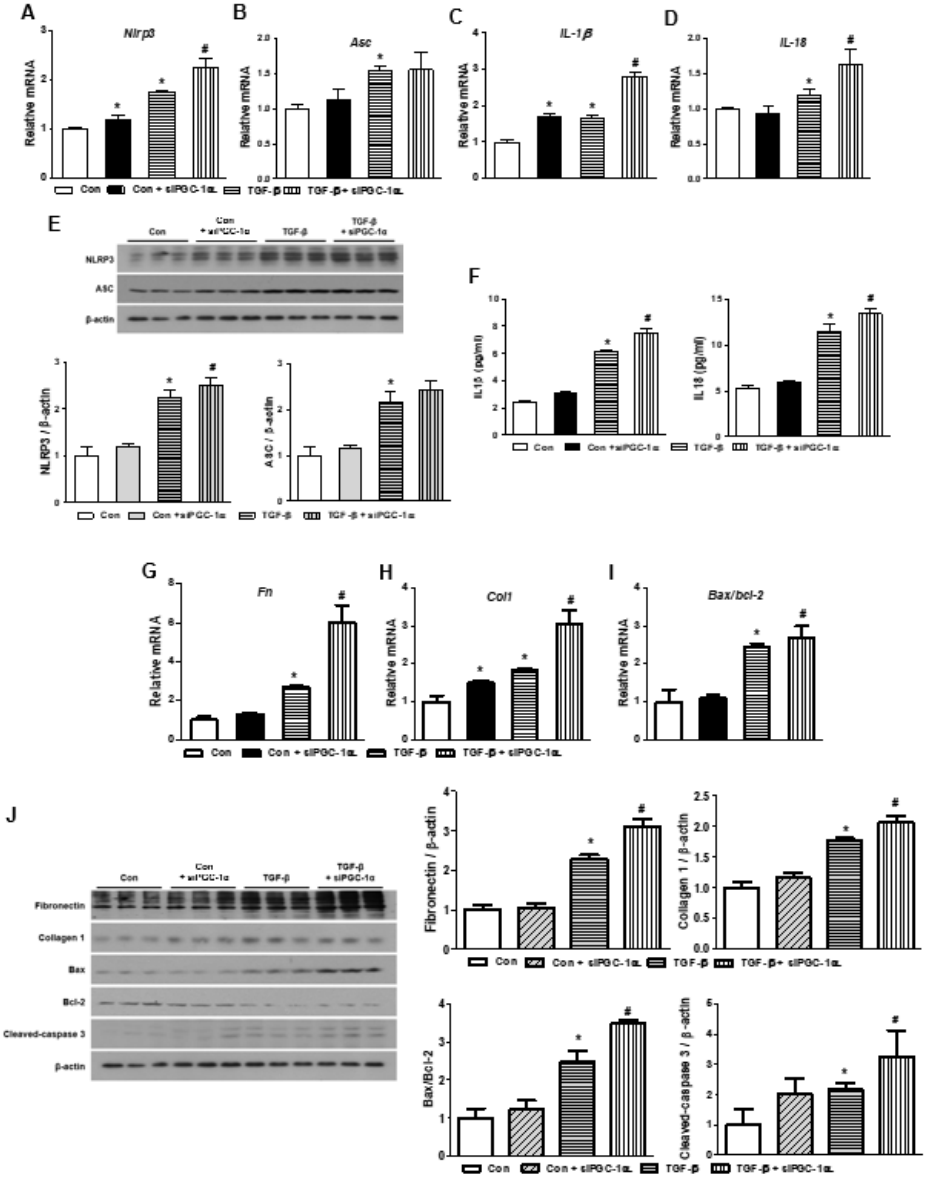

Figure 9. Downregulation of PGC-1α gene exacerbates cell injury with activation of NLRP3 inflammasome. (A-D) mRNA and **(E)** protein expression levels of NLRP3 inflammasome pathway and **(F)** concentrations of IL-1β and IL-18 assessed by ELISA were increased in TGF-β1-treated RTECs with siPGC-1α. **(G-I)** mRNA and **(J)** protein expression levels of fibrotic and apoptotic markers

were enhanced in TGF-β1-treated RTECs with siPGC-1α.

Note: * $P<0.05$ vs. control; # $P<0.05$ vs. TGF-β1-treated RTEC.

Abbreviations: PGC-1α, peroxisomal proliferator-γ coactivator-1α; NLRP3, NOD-like receptor family, pyrin domain-containing 3; RTEC, renal tubular epithelial cell; Met, metformin; siRNA, small interfering RNA.

4. Dysregulated mitochondria-induced oxidative stress and PGC-1α/TNFAIP3 axis regulate NLRP3 inflammasome

Because oxidative stress is a positive regulator of NLRP3 inflammasome and its level is increased upon mitochondrial damage, I examined markers of oxidative stress in TGF-β1-treated cells with or without PGC-1α. TGF-β1 increased MitoSOX staining intensity and MDA levels in RTECs and PGC-1α activators and direct PGC-1α overexpression attenuated this overproduction of mitochondrial ROS (**Fig. 10A**). Conversely, PGC-1α knock-down further increased MDA levels in TGF-β1-treated RTECs (**Fig. 10B**). Then, I further examined TNFAIP3, which is regulated by PGC-1α and also known as a negative regulator of NLRP3 inflammasome. TGF-β1 reduced transcript levels of *Tnfaip3* and this decreased expression of *Tnfaip3* was restored by restoration of PGC-1α. Conversely, PGC-1α knock-down resulted in further decreased expression of *Tnfaip3* (**Fig. 10C**). These findings suggest that PGC-1α can regulate NLRP3 inflammasome via modulation of mitochondrial ROS/oxidative stress and TNFAIP3.

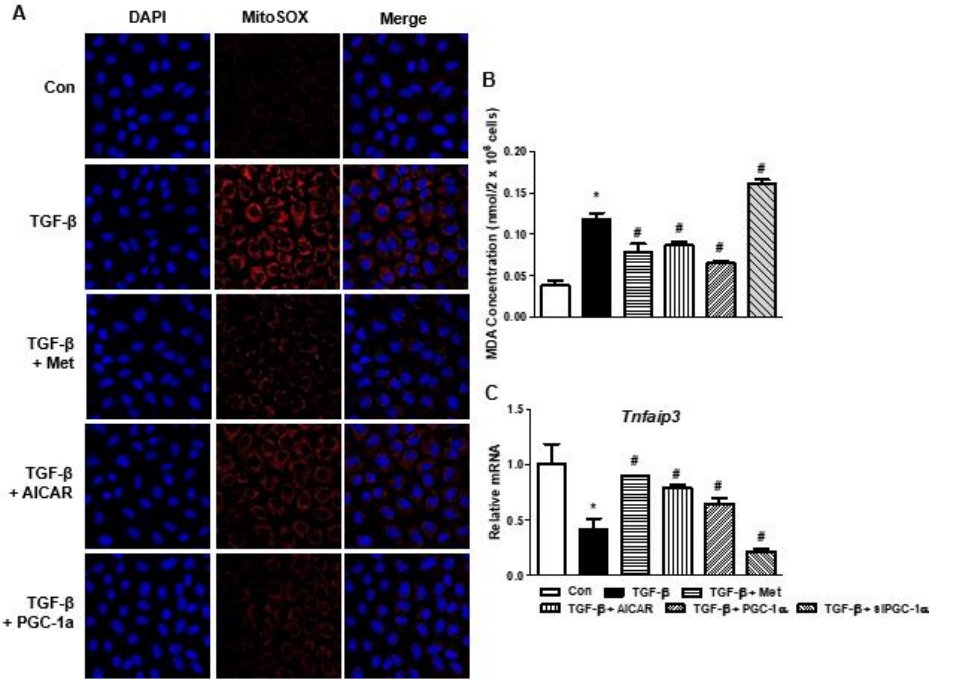

Figure 10. Dysregulated mitochondria-induced oxidative stress and PGC-1α/TNFAIP3 axis regulate NLRP3 inflammasome. (A) Confocal microscopy analysis with MitoSOX staining revealed increased production of mitochondria-generated ROS in TGF-β1-treated RTECs, which were reduced with PGC-1α activators and transfection of PGC-1α plasmid. **(B)** Measurement of oxidative stress levels by MDA showed reduction of oxidative stress levels in TGF-β1-treated RTECs with PGC-1α activators and transfection of PGC-1α plasmid, which were increased by siPGC-1α. **(C)** mRNA expression level of TNFAIP3 in TGF-β1-treated RTECs was increased with PGC-1α activators and transfection of PGC-1α plasmid, which were reduced by siPGC-1α.

Note: * P<0.05 vs. control; # P<0.05 vs. TGF-β-treated RTECs.

Abbreviations: PGC-1α, peroxisomal proliferator-γ coactivator-1α; ROS, reactive oxygen species; RTEC; renal tubular epithelial cell; TNFAIP3, tumor necrosis factor α induced protein 3; NLRP3, NOD-like receptor family, pyrin domain-containing 3; MDA, malondialdehyde; Met, metformin; AICAR, 5-

aminoimidazole-4-carboxamide ribonucleotide; siRNA, small interfering RNA.

5. PGC-1α protects kidney fibrosis and attenuates mitochondrial damage and activation of NLRP3 inflammasome in adenine-fed animal model

To confirm the findings of in vitro study, I tested the effects of metformin, a PGC1α activator, using adenine-induced kidney injury model. In the kidney of adenine-fed mice, expression level of TGF-β1 was increased, while that of PGC-1α was decreased (**Fig. 11A and B**). In addition, there were altered expression of mitochondria dynamic-related genes in these mice; the decreased expression levels of *Mfn* and *Tfam* and the increased expression of *Drp1* (**Fig. 11C-E**). Treatment with metformin, restored the decreased expression of PGC-1α and reversed the altered expression of mitochondrial dynamic-related genes in adenine-fed mice (**Fig. 11A-E**). Electron microscopy examination also confirmed the loss of mitochondria integrity in TECs of adenine-fed mice. These were significantly improved by PGC-1α activator (**Fig. 11F**). Moreover, the increased expression levels of NLRP3 inflammasome pathway components were concomitantly decreased by PGC-1α activator (**Fig. 12A-E**). The concentrations of IL-1β and IL-18, the final products of NLRP3 pathway, were significantly decreased by metformin treatment (**Fig. 12F**).

Oligomerization of NLRP3 with the adapter protein, ASC, is a key step of inflammasome complex formation. Thus, I examined whether the assembly of NLRP3 inflammasome is affected by PGC-1α in animal model. In adenine-fed mice, NLRP3 oligomerization and activation was confirmed by ASC binding to NLRP3 and this was abolished by PGC-1α activator (**Fig. 12G**). In aggregates, these findings indicate that the assembly of NLRP3 inflammasome complex was induced during kidney injury, and the activation of this pathway was attenuated by PGC-1α activator.

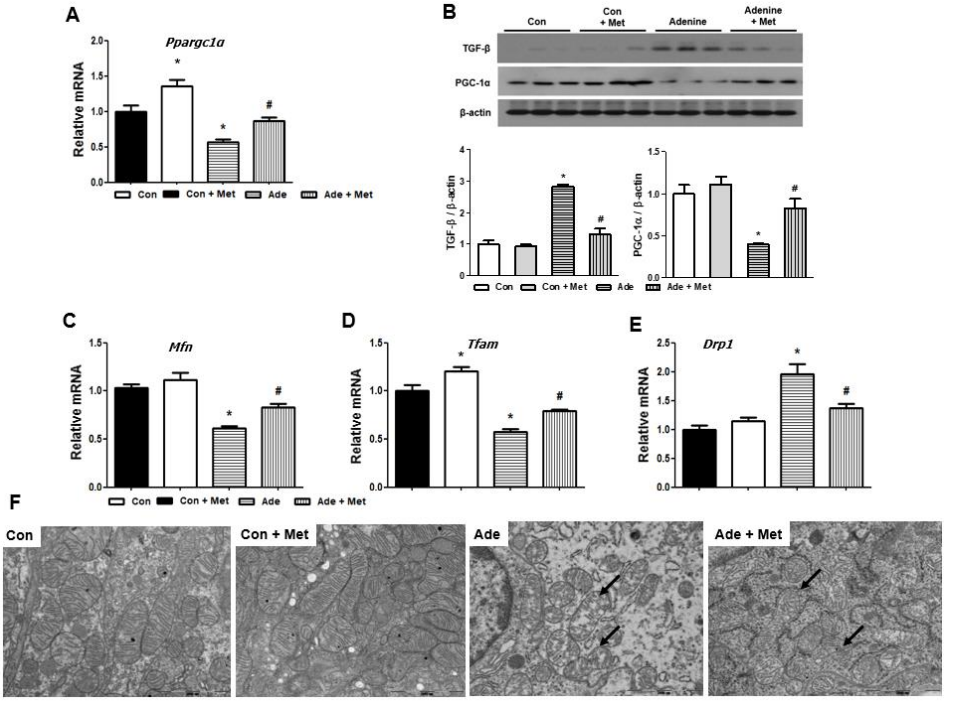

Figure 11. PGC-1α activator protects mitochondrial damage in adenine-fed animal model. (A) mRNA and **(B)** protein expression levels of PGC-1α in adenine-fed mice were increased with PGC-1α activator. **(C-E)** mRNA expression levels of mitochondrial dynamic-related genes were restored in adenine-fed mice with PGC-1α activator. **(F)** Transmission electron microscopy images of RTECs from adenine-fed mice showed restoration of mitochondrial structures with PGC-1α activator.

Note: * P<0.05 vs. control; # P<0.05 vs. Adenine.

Abbreviations: PGC-1α, peroxisomal proliferator-γ coactivator-1α; NLRP3, NOD-like receptor family, pyrin domain-containing 3; Ade, adenine; Met, metformin; Mfn, mitofusin; Tfam, mitochondrial transcriptional factor A; Drp1, dynamin related protein 1.

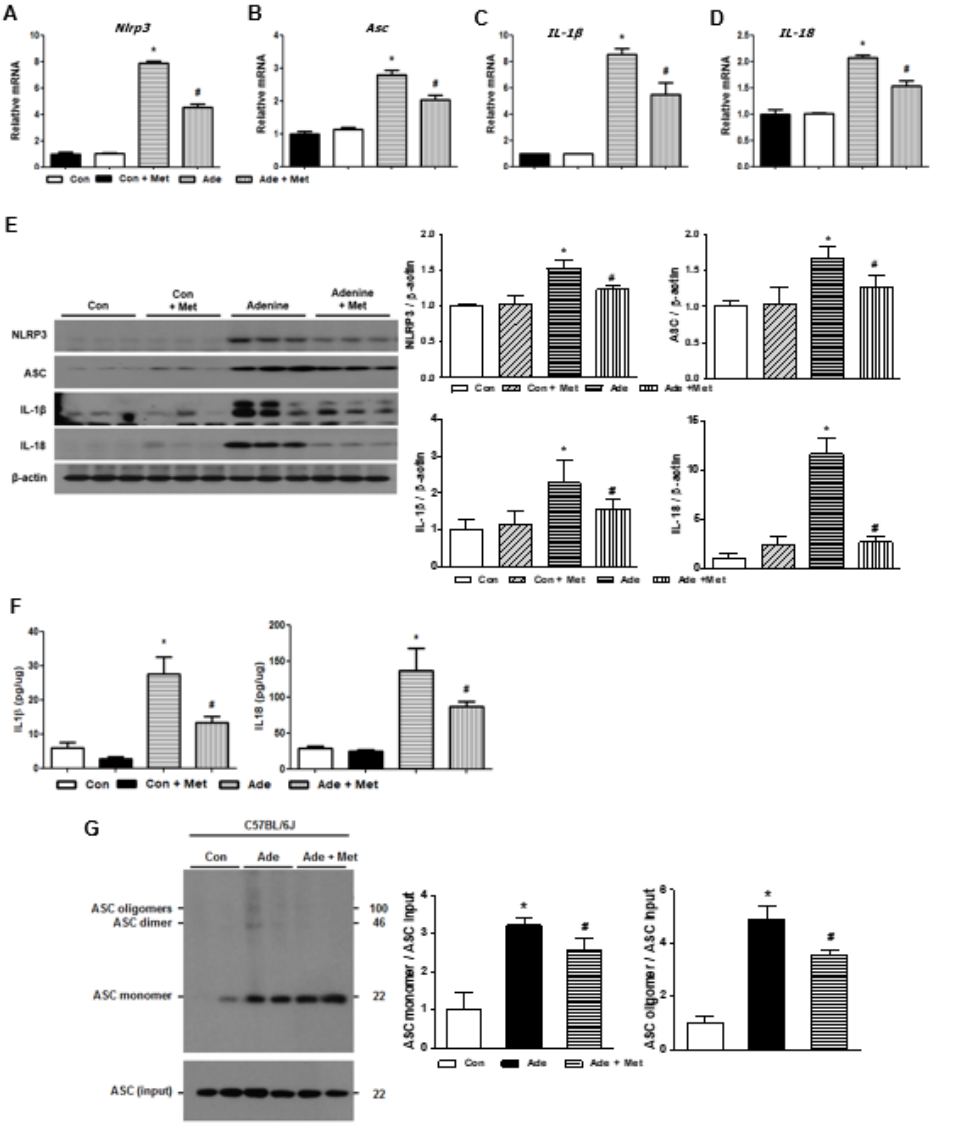

Figure 12. PGC-1α activator protects cell injury and attenuates oligomerization and activation of NLRP3 inflammasome in adenine-fed animal model. (A-D) mRNA and **(E)** protein expression levels of NLRP3 inflammasome pathway in adenine-fed mice were reduced with PGC-1α activator. **(F)** Concentration of IL-1β and IL-18 in kidney tissues measured by ELISA were decreased in adenine-fed mice with PGC-1α activator. **(G)** ASC oligomeric

structures assayed by DSS-mediated cross-linking were observed in adenine-fed mice, which were attenuated with PGC-1α activator.

Note: * $P<0.05$ vs. control; # $P<0.05$ vs. Adenine.

Abbreviations: PGC-1α, peroxisomal proliferator–γ coactivator-1α; NLRP3, NOD-like receptor family, pyrin domain-containing 3; ASC, apoptosis-associated speck-like protein containing a caspase recruitment domain; Ade, adenine; Met, metformin; ELISA, enzyme-linked immunosorbent assay; DSS, disuccinimidyl suberate.

6. PGC-1α activator regulates TNFAIP3 associated NLRP3 inflammasome activation with oxidative stress and protects kidney fibrosis in adenine-fed animal model

Similar to the findings of in vitro study, MDA levels were significantly increased in adenine-fed mice. The enhanced oxidative stress was largely reduced by PGC-1α activator (**Fig. 13A**). In contrast, there was a decreased expression of TNFAIP3 in adenine-fed mice and PGC-1α activator restored this expression (**Fig. 13B and C**). In accordance with these findings, the expression levels of fibrotic markers and apoptotic cell death index were significantly increased in these mice. In contrast, PGC-1α activator reversed all these findings (**Fig. 14A-D**). Together with these findings, the degree of kidney fibrosis was also reduced after treatment of metformin to adenine-fed mice (**Fig. 14E**).

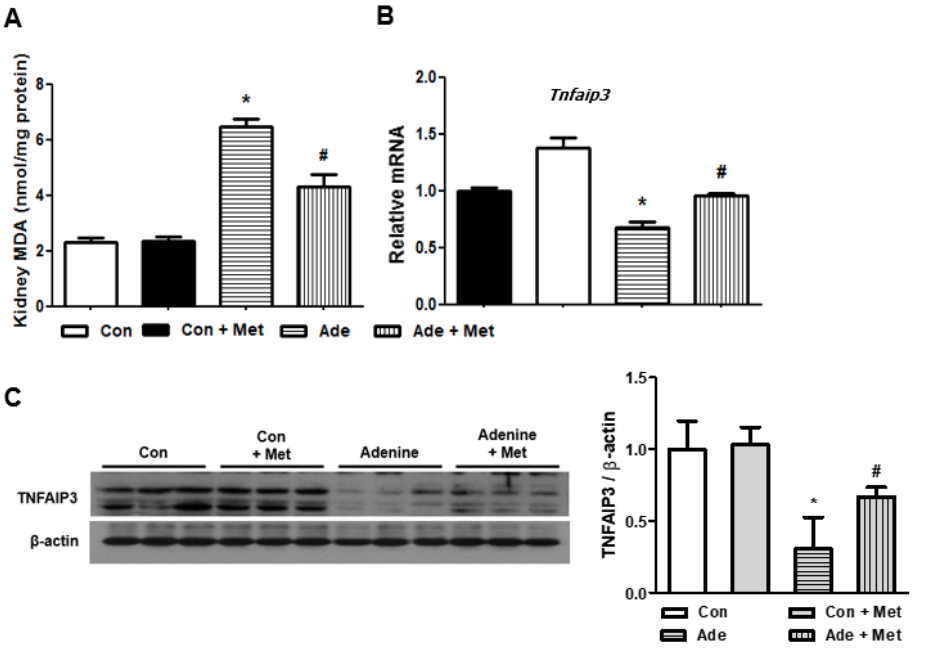

Figure 13. PGC-1α activator regulates TNFAIP3 associated NLRP3 inflammasome activation with oxidative stress in adenine-fed animal model. **(A)** The oxidative stress levels measured by MDA were reduced in adenine-fed mice with PGC-1α activator. **(B)** mRNA and protein **(C)** expression levels of TNFAIP3 were restored in adenine-fed mice with PGC-1α activator.

Note: * $P<0.05$ vs. control; # $P<0.05$ vs. Adenine.

Abbreviations: PGC-1α, peroxisomal proliferator–γ coactivator-1α; TNFAIP3, tumor necrosis factor α induced protein 3; NLRP3, NOD-like receptor family, pyrin domain-containing 3; MDA, malondialdehyde; Met, metformin.

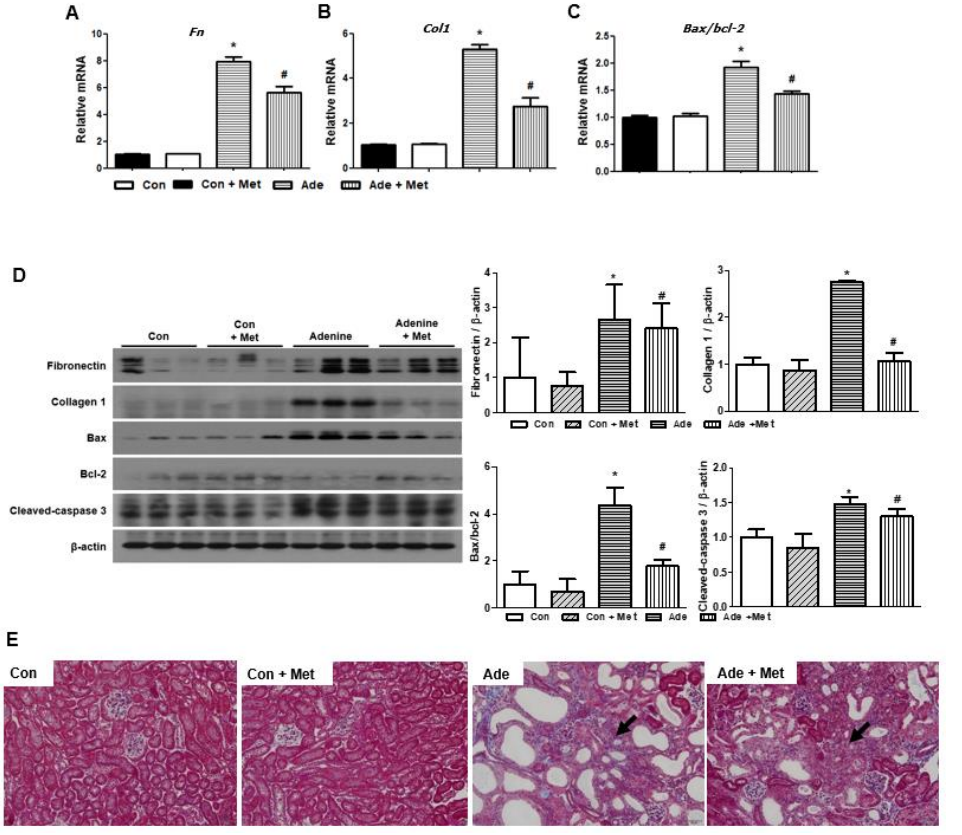

Figure 14. PGC-1α activator protects kidney fibrosis in adenine-fed animal model.

(A-C) mRNA and **(D)** protein expression levels of fibrotic and apoptotic markers were reduced in adenine-fed mice with PGC-1α activator. **(E)** Degree of kidney fibrosis by Masson's trichrome staining were attenuated in adenine-fed mice with PGC-1α activator.

Note: * P<0.05 vs. control; # P<0.05 vs. Adenine.

Abbreviations: PGC-1α, peroxisomal proliferator-γ coactivator-1α; NLRP3, NOD-like receptor family, pyrin domain-containing 3; Ade, adenine; Met, metformin

7. PGC-1α protects kidney fibrosis and attenuates mitochondrial damage and activation of NLRP3 inflammasome in UUO model

To substantiate my findings, I additionally performed experimental study using different renal tubular injury model, unilateral ureteral obstruction (UUO) model. Similar to the findings in adenine-fed animal model above, I also observed the altered expression levels of PGC-1α and mitochondrial dynamic-related genes in UUO mice. In contrast, PGC-1α activators reversed all these findings (**Fig. 15A-E**). Electron microscopy examination also confirmed the loss of mitochondria integrity in RTECs of UUO mice. These were significantly improved by PGC-1α activators (**Fig. 15F**). Moreover, the expression levels of NLRP3 inflammasome pathway and MDA levels were increased, whereas the expression of TNFAIP3 was decreased in these mice (**Fig. 16A-G**). Along with these findings, fibrotic and apoptotic markers were also increased (**Fig. 16H-K**). However, PGC-1α activators reversed all these findings (**Fig. 16A-K**).

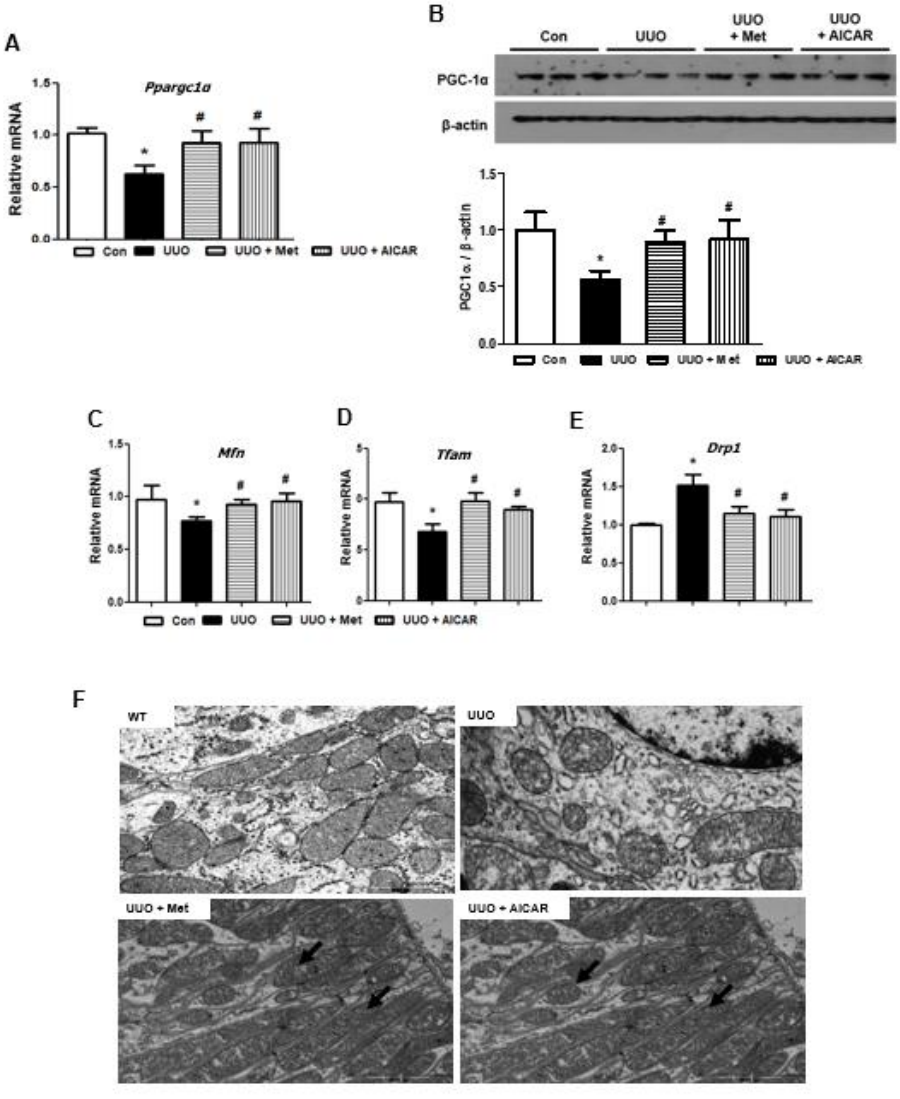

Figure 15. PGC-1α activators attenuates mitochondrial damage in UUO animal model. (A) mRNA and **(B)** protein expression levels of PGC-1α were increased in UUO mice with PGC-1α activators. **(C-E)** mRNA expression levels of mitochondrial dynamic-related genes in UUO mice were restored with PGC-1α activators. **(F)** Transmission electron microscopy images of RTECs from UUO mice showed restoration of mitochondrial structure with PGC-1α activators.
Note: * $P<0.05$ vs. control; # $P<0.05$ vs. UUO.

Abbreviations: PGC-1α, peroxisomal proliferator-γ coactivator-1α; NLRP3, NOD-like receptor family, pyrin domain-containing 3; UUO, unilateral ureteral obstruction; Met, metformin; AICAR, 5-aminoimidazole-4-carboxamide ribonucleotide; Mfn, mitofusin; Drp1, dynamin related protein 1; Tfam, mitochondrial transcriptional factor A.

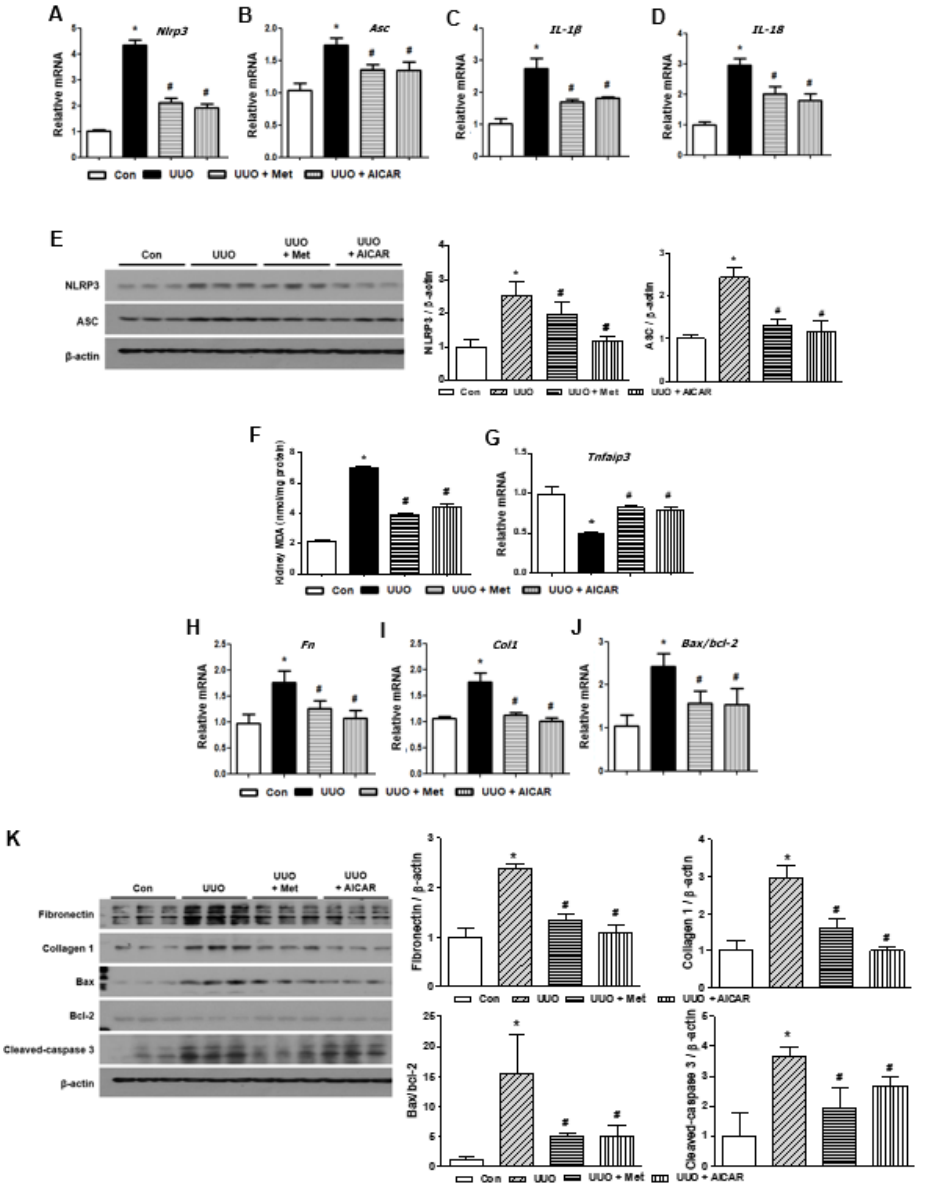

Figure 16. PGC-1α activator protects kidney fibrosis and attenuates activation of NLRP3 inflammasome in UUO animal model. (A-D) mRNA and **(E)** protein expression levels of NLRP3 inflammasome pathway in UUO mice were reduced with PGC-1α activator. **(F)** Decreased oxidative stress levels by MDA were observed in UUO mice with PGC-1α activator. **(G)** mRNA

expression level of TNFAIP3 in UUO was increased with PGC-1α activators. (**H-J**) mRNA and (**K**) protein expression levels of fibrotic and apoptotic markers in UUO mice were reduced with PGC-1α activators.

Note: * $P<0.05$ vs. control; # $P<0.05$ vs. UUO.

Abbreviations: PGC-1α, peroxisomal proliferator-γ coactivator-1α; NLRP3, NOD-like receptor family, pyrin domain-containing 3; UUO, unilateral ureteral obstruction; Met, metformin; AICAR, 5-aminoimidazole-4-carboxamide ribonucleotide; MDA, malondialdehyde; TNFAIP3, tumor necrosis factor α induced protein 3.

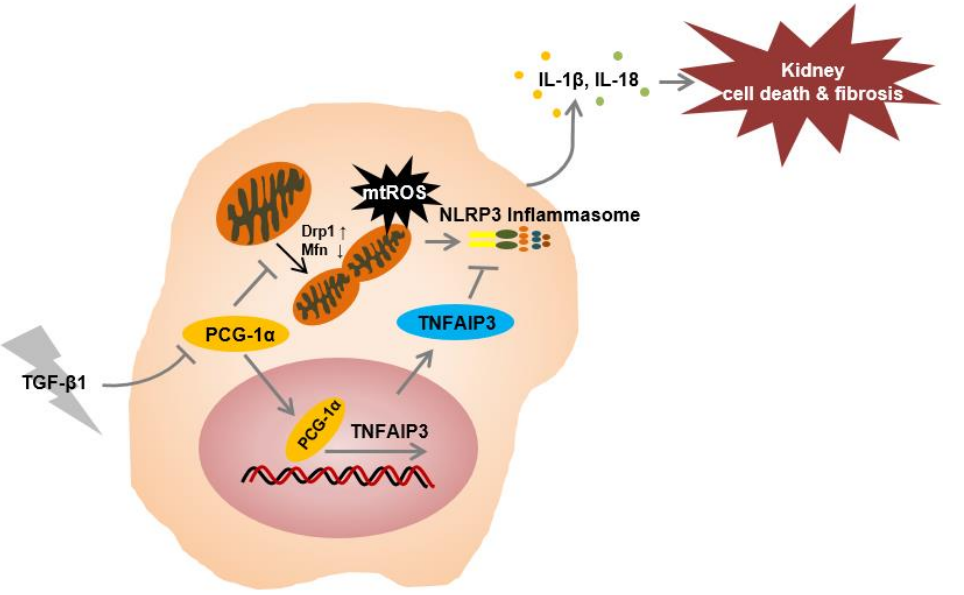

Figure 17. Schematic summary. PGC-1α regulates the NLRP3 inflammasome activation via modulating mitochondrial viability and dynamics, and TNFAIP3 during kidney cell death and fibrosis.

Abbreviations: PGC-1α, peroxisomal proliferator–γ coactivator-1α; NLRP3, NOD-like receptor family, pyrin domain-containing 3 TNFAIP3, tumor necrosis factor α induced protein 3; Mfn, mitofusin; Drp1, dynamin related protein 1.

IV. DISCUSSION

The present study showed that PGC-1α decreased mitochondrial damage and oxidative stress levels, restored mitochondrial integrity and TNFAIP3, and attenuated the activation of NLRP3 inflammasome pathway in TGF-β-treated RTECs and animal models of kidney injury. These improvements concomitantly resulted in decreased cell injury and fibrosis. A schematic figure showing the potential mechanism on regulation of NLRP3 by PGC-1α is presented in **Figure 17**. The findings of my study unravel the role of PGC-1α in the regulation of the

NLRP3 inflammasome signaling via modulating mitochondrial viability and dynamics and also suggest a possible therapeutic potential of PGC-1α during kidney injury.

The NLRP3 inflammasome has been implicated in the pathogenesis of cellular injury, inflammation, and fibrosis in various kidney injury models.[13-18,27,28] A previous study by Vilaysane et al. [13] showed that the expression levels of markers of inflammasome activation such as caspase-1, IL-1β, and IL-18 were increased in mice after UUO. Genetic deletion of *Nlrp3* in these mice markedly decreased inflammation and tubular injury. Furthermore, these NLRP3 Inflammasome-regulated cytokines such as IL-1β and IL-18 induced mesenchymal markers in RTECs in a dose dependent manner.[17,29] In contrast, IL-18 neutralization substantially prevented renal tubular injury and fibrosis. Interestingly, in a cohort of renal biopsies from patients with kidney disease, the increased expression levels of NLRP3 well correlated with decreased renal function. In addition, markers of inflammasome signaling such as IL-18 and caspase-1 were expressed in human kidney disease,[30] and circulating IL-18 levels were elevated in patients with CKD or nephrotic syndrome.[31-33] These findings suggest that NLRP3 may play a role in human kidney disease.

In agreement with previous studies, I showed that the expression levels of NLRP3 inflammasome pathways including NLRP3, ASC, IL-1β, and IL-18 were increased along with elevated expression levels of cellular injury markers during kidney injury in TGF-β1-treated RTECs and animal models with adenine-diet and UUO. Several damage-associated molecular patterns (DAMPs) released during renal tubular cell injury are suggested to activate the NLRP3 inflammasome.[34] These DAMPs include ROSs, extracellular ATP, uric acid, nucleic acids, and extracellular matrix components such as hyaluronan and biglycan.[27,35-41] Notably, kidney intrinsic cells express components of NLRP3 inflammasome pathway,[42] and activation of this signaling can contribute to kidney injury.[13,28] However, it is uncertain how NLRP3 is activated in these cells.

In this study, I particularly focused on regulators of mitochondrial biogenesis because dysregulated mitochondria can trigger the activation of NLRP3 inflammasome pathway.[43,44]

PGC-1α is a key regulator of mitochondrial biogenesis and plays an important role in mitochondrial dynamics and mitophagy.[45-47] Given the relative abundance of mitochondria found in the kidney compared with other organs, growing attention has been paid to PGC-1α in kidney disease research field. In the kidney, PGC-1α expression is localized to the cortex and outer medulla, corresponding with regions of high mitochondrial activity.[48] As damaged mitochondria are apparently observed in various forms of acute kidney injury (AKI), several studies have demonstrated the crucial protective role of PGC-1α against AKI.[48] Furthermore, there has been accumulating evidence that loss of PGC-1α contributes to the development of renal fibrosis and subsequent CKD.[9,49,50] Portilla et al.[51] indicated that PGC-1α plays a role in the regulation of fatty acid oxidation during cisplatin-induced AKI model. Furthermore, transcript levels of *Ppargc1α* were notably decreased in patients with CKD compared with controls.[52] The mRNA expression of *Ppargc1α* was significantly reduced in models of UUO–, folic acid–and APOL1-induced kidney fibrosis models. Most recently, in Notch-induced kidney injury model, PGC-1α also protected tubule injury and ameliorated fibrosis.[9] Here, I demonstrated the role of PGC-1α in preventing kidney injury in light of regulation of NLRP3 pathway. Direct or indirect overexpression of PGC-1α attenuated TGF-β1-induced cell damage as well as activation of NLRP3 inflammasome. These results were consistent with animal models such as adenine-diet and UUO models. In adenine-fed mice, treatment of PGC-1α activators decreased oligomerization of NLRP3-ASC inflammasome. Conversely, down-regulation of PGC-1α augmented TGF-β1-induced the activation of NLRP3 inflammasome and cellular injury.

To date, few studies have examined the relationship between PGC-1α and NLRP3. In a study by Diao et al.,[53] severe burn injury induced endoplasmic

reticulum (ER) stress in hepatocytes, and in turn activated NLRP3 inflammasome. Interestingly, activation of hepatic NLRP3 inflammasome was in parallel with inhibition of PGC-1α. They further examined the upstream regulators of PGC-1α such as protein kinase A catalyst, AMP-activated protein kinase, and sirtuin-1, all of which were significantly decreased after burn injury. They suggested that lack of PGC-1α may play an important role in the metabolic derangement and contributes to the activation of NLRP3 inflammasome pathway. To my knowledge, this is the first study that clarified the relationship on PGC-1α/NLRP3 axis in RTECs.

In the present study, I demonstrated several mechanisms that PGC-1α regulates NLRP3 inflammasome pathway in the kidney. Mitochondria are the powerhouse of the cell, and they play an important role in cellular homeostasis.[54] Because RTECs have high energy–demanding function, mitochondrial dysfunction and reduced energy supply have been described in patients and animal models of CKD.[55] Dysfunctional mitochondria eventually imperil cell viability, leading to cell death and dedifferentiation.[56,57] PGC-1α orchestrates mitochondrial biogenesis by interacting with estrogen-related receptor-α, peroxisome proliferator–activated receptors, and nuclear respiratory factors 1 and 2, thereby increasing mitochondrial mass and overall mitochondrial function.[58-60] Given that PGC-1α plays a key role in regulating mitochondrial biogenesis and mitochondrial dynamics, it can be suggested that PGC-1α regulates NLRP3 inflammasome pathway via modulating mitochondrial viability. As shown in my data, the expression levels of mitochondrial dynamic-related genes were dysregulated in TGF-β1-treated RTECs. These changes were restored by direct or indirect overexpression of PGC-1α, while down-regulation of PGC-1α aggravated this dysregulation. The structural improvement of TGF-β1-induced mitochondria damage by PGC-1α were also observed by MitoTracker staining. In addition, transmission electron microscopy showed that destruction of mitochondrial structure by adenine diet-induced or UUO-induced kidney injury

was also restored by PGC-1α activators. Finally, I showed the release of mtDNA to cytosol from mitochondrial fraction in TGF-β1-treated RTECs. This release of mtDNA was prevented by PGC-1α overexpression. These findings together suggest that dysregulated mitochondrial dynamics contribute to the activation of NLRP3 inflammasome and consequent renal tubulointerstitial inflammation and fibrosis.

PGC-1α also has critical roles in essential metabolic processes such as fatty acid oxidation, oxidative phosphorylation, and ROS detoxification.[57,61,62] In addition, several NLRP3-activating stimuli are associated with ROS production.[36] Thus, regulation of oxidative stress levels by PGC-1α can affect NLRP3 inflammasome activation. Recently, mitochondrial ROS production has been described to trigger activation of NLRP3 inflammasome during renal tubulointerstitial fibrosis. Zhuang et al.[21] reported that mitochondria-derived oxidative stress had key role in mediating the albumin effect on mitochondrial dysfunction and subsequent renal tubular injury. Furthermore, NLRP3 inflammasome was activated in the kidney by albumin overload, which was entirely abolished by MnTBAP, a mitochondrial ROS scavenger. In line with these study, I showed that enhanced oxidative stress was associated with the activation of NLRP3 inflammasome pathway during kidney injury. This increased oxidative stress level was attenuated by direct or indirect or direct overexpression of PGC-1α, whereas augmented after down-regulation of PGC-1α. The reduction of oxidative stress levels by PGC-1α activators was also confirmed in two different animal models. Taken together, enhanced oxidative stress levels including mitochondrial ROS production by PGC-1α deficiency can result in the activation of NLRP3 inflammasome and consequent renal tubulointerstitial inflammation and fibrosis.

TNFAIP3 is known to be directly regulated by PGC-1α and it has a role in inactivating NLRP3 inflammasome pathway in inflammatory cells such as macrophage. Kang et al.[63] showed that dysfunctional telomeres cause macrophage mitochondrial distress, metabolic imbalance, and hyperactivation of

the NLRP3 inflammasome. They identified the PGC-1α/TNFAIP3 axis as a mechanism responsible for the homeostatic role of the telomere, and the disturbance of this axis led to inflammatory $Terc^{-/-}$ macrophages and severe bacterial pneumonia in $Terc^{-/-}$ mice. In the present study, TGF-β1 decreased transcript level of *Tnfaip3* in RTECs. PGC-1α restored these changes, whereas PGC-1α knock-down further decreased *Tnfaip3* level. Thus, PGC-1α /TNFAIP3 axis is involved in regulation of NLRP3 inflammasome pathway in RTECs.

This study has several limitations. I did not use PGC-1α knock-out animal model in the present study due to infeasibility of proper genetic mouse model, the association between PGC-1α, mitochondrial biogenesis, and NLRP3 inflammasome could not be clearly demonstrated *in vivo*. However, I thoroughly evaluated this relationship *in vitro* using various methods including the use of PGC-1α activators, and delivery or knockdown of PGC-1α. Second, kidney tissue obtained from animal models included both cortex and medulla. Thus, the renal tubule cell-specific effects of PGC-1α on mitochondria, and NLRP3 inflammasome were not clear. In addition, possible involvement of other type of cells such as macrophage in kidney injury, which play an important role in activating NLRP3 inflammasome pathway, was not studied. However, RTECs constitutes 90% of the whole kidney and tubular cell death can trigger subsequent kidney injury. Thus, identifying the relationship between PGC-1α and NLRP3 in these cells is meaningful. Finally, metformin, which is known as PGC-1α activator, may have opposite effect on mitochondrial viability. Metformin modifies the production of ROSs and affects cell death processes, especially in cancer cells, which it has been also implicated in anti-neoplastic therapy.[64] Most of these effects are caused by inhibiting complex 1 of mitochondrial respiratory chain.[65] However, metformin is less toxic in non-cancer cells and it is possible that biologic effects of metformin differ between cancer and non-cancer cells. Future studies are warranted to uncover the direct effect of PGC-1α and its activating drugs on NLRP3 inflammasome and renal fibrosis process.

V. CONCLUSION

In the present study, I demonstrated the role of PGC-1α in the regulation of the NLRP3 inflammasome activation via modulating mitochondrial dynamics and viability, and TNFIP3 during kidney injury. These results suggest that inhibition of NLRP3 inflammasome by PGC-1α can be a future therapeutic target against CKD.

REFERENCES

1. Saran R, Robinson B, Abbott KC, Agodoa LYC, Bragg-Gresham J, Balkrishnan R, et al. US Renal Data System 2018 Annual Data Report: Epidemiology of Kidney Disease in the United States. Am J Kidney Dis 2019;73:A7-a8.
2. Coresh J, Selvin E, Stevens LA, Manzi J, Kusek JW, Eggers P, et al. Prevalence of chronic kidney disease in the United States. Jama 2007;298:2038-47.
3. Levey AS, Atkins R, Coresh J, Cohen EP, Collins AJ, Eckardt KU, et al. Chronic kidney disease as a global public health problem: approaches and initiatives - a position statement from Kidney Disease Improving Global Outcomes. Kidney Int 2007;72:247-59.
4. Tonelli M, Wiebe N, Culleton B, House A, Rabbat C, Fok M, et al. Chronic kidney disease and mortality risk: a systematic review. J Am Soc Nephrol 2006;17:2034-47.
5. Park S, Lee S, Jo HA, Han K, Kim Y, An JN, et al. Epidemiology of continuous renal replacement therapy in Korea: Results from the National Health Insurance Service claims database from 2005 to 2016. Kidney Res Clin Pract 2018;37:119-29.
6. Boor P, Ostendorf T, Floege J. Renal fibrosis: novel insights into mechanisms and therapeutic targets. Nat Rev Nephrol 2010;6:643-56.
7. Liu BC, Tang TT, Lv LL, Lan HY. Renal tubule injury: a driving force toward chronic kidney disease. Kidney Int 2018;93:568-79.
8. Galvan DL, Green NH, Danesh FR. The hallmarks of mitochondrial dysfunction in chronic kidney disease. Kidney Int 2017;92:1051-7.
9. Han SH, Wu MY, Nam BY, Park JT, Yoo TH, Kang SW, et al. PGC-1alpha Protects from Notch-Induced Kidney Fibrosis Development. J Am Soc Nephrol 2017;28:3312-22.
10. Ting JP, Lovering RC, Alnemri ES, Bertin J, Boss JM, Davis BK, et al.

The NLR gene family: a standard nomenclature. Immunity 2008;28:285-7.

11. Lech M, Avila-Ferrufino A, Skuginna V, Susanti HE, Anders HJ. Quantitative expression of RIG-like helicase, NOD-like receptor and inflammasome-related mRNAs in humans and mice. Int Immunol 2010;22:717-28.
12. Rathinam VA, Vanaja SK, Fitzgerald KA. Regulation of inflammasome signaling. Nat Immunol 2012;13:333-42.
13. Vilaysane A, Chun J, Seamone ME, Wang W, Chin R, Hirota S, et al. The NLRP3 inflammasome promotes renal inflammation and contributes to CKD. J Am Soc Nephrol 2010;21:1732-44.
14. Hutton HL, Ooi JD, Holdsworth SR, Kitching AR. The NLRP3 inflammasome in kidney disease and autoimmunity. Nephrology (Carlton) 2016;21:736-44.
15. Lorenz G, Darisipudi MN, Anders HJ. Canonical and non-canonical effects of the NLRP3 inflammasome in kidney inflammation and fibrosis. Nephrol Dial Transplant 2014;29:41-8.
16. Vesey DA, Cheung CW, Cuttle L, Endre ZA, Gobe G, Johnson DW. Interleukin-1beta induces human proximal tubule cell injury, alpha-smooth muscle actin expression and fibronectin production. Kidney Int 2002;62:31-40.
17. Vesey DA, Cheung C, Cuttle L, Endre Z, Gobe G, Johnson DW. Interleukin-1beta stimulates human renal fibroblast proliferation and matrix protein production by means of a transforming growth factor-beta-dependent mechanism. J Lab Clin Med 2002;140:342-50.
18. Bani-Hani AH, Leslie JA, Asanuma H, Dinarello CA, Campbell MT, Meldrum DR, et al. IL-18 neutralization ameliorates obstruction-induced epithelial-mesenchymal transition and renal fibrosis. Kidney Int 2009;76:500-11.

19. Chun J, Chung H, Wang X, Barry R, Taheri ZM, Platnich JM, et al. NLRP3 Localizes to the Tubular Epithelium in Human Kidney and Correlates With Outcome in IgA Nephropathy. Sci Rep 2016;6:24667.
20. Bai M, Chen Y, Zhao M, Zhang Y, He JC, Huang S, et al. NLRP3 inflammasome activation contributes to aldosterone-induced podocyte injury. Am J Physiol Renal Physiol 2017;312:F556-f64.
21. Zhuang Y, Yasinta M, Hu C, Zhao M, Ding G, Bai M, et al. Mitochondrial dysfunction confers albumin-induced NLRP3 inflammasome activation and renal tubular injury. Am J Physiol Renal Physiol 2015;308:F857-66.
22. Hsu WH, Hua KF, Tuan LH, Tsai YL, Chu LJ, Lee YC, et al. Compound K inhibits priming and mitochondria-associated activating signals of NLRP3 inflammasome in renal tubulointerstitial lesions. Nephrol Dial Transplant 2019; doi:10.1093/ndt/gfz073.
23. Xu Y, Wang J, Xu W, Ding F, Ding W. Prohibitin 2-mediated mitophagy attenuates renal tubular epithelial cells injury by regulating mitochondrial dysfunction and NLRP3 inflammasome activation. Am J Physiol Renal Physiol 2019;316:F396-f407.
24. Ding Y, Kim S, Lee SY, Koo JK, Wang Z, Choi ME. Autophagy regulates TGF-beta expression and suppresses kidney fibrosis induced by unilateral ureteral obstruction. J Am Soc Nephrol 2014;25:2835-46.
25. Fernandes-Alnemri T, Yu JW, Juliana C, Solorzano L, Kang S, Wu J, et al. The AIM2 inflammasome is critical for innate immunity to Francisella tularensis. Nat Immunol 2010;11:385-93.
26. Biovision Inc. Mitochondrial DNA Isolation Kit. Available: http://www.biovision.com/mitochondrial-dna-isolation-kit-2835.html. See PDF Data Sheet in Product Toolbox. 2015.
27. Babelova A, Moreth K, Tsalastra-Greul W, Zeng-Brouwers J, Eickelberg O, Young MF, et al. Biglycan, a danger signal that activates the NLRP3

inflammasome via toll-like and P2X receptors. J Biol Chem 2009;284:24035-48.

28. Anders HJ, Muruve DA. The inflammasomes in kidney disease. J Am Soc Nephrol 2011;22:1007-18.
29. Liang D, Liu HF, Yao CW, Liu HY, Huang-Fu CM, Chen XW, et al. Effects of interleukin 18 on injury and activation of human proximal tubular epithelial cells. Nephrology (Carlton) 2007;12:53-61.
30. Gauer S, Sichler O, Obermuller N, Holzmann Y, Kiss E, Sobkowiak E, et al. IL-18 is expressed in the intercalated cell of human kidney. Kidney Int 2007;72:1081-7.
31. Matsumoto K, Kanmatsuse K. Elevated interleukin-18 levels in the urine of nephrotic patients. Nephron 2001;88:334-9.
32. Matsumoto K, Kanmatsuse K. Augmented interleukin-18 production by peripheral blood monocytes in patients with minimal-change nephrotic syndrome. Am J Nephrol 2001;21:20-7.
33. Lonnemann G, Novick D, Rubinstein M, Dinarello CA. Interleukin-18, interleukin-18 binding protein and impaired production of interferon-gamma in chronic renal failure. Clin Nephrol 2003;60:327-34.
34. Masters SL, Simon A, Aksentijevich I, Kastner DL. Horror autoinflammaticus: the molecular pathophysiology of autoinflammatory disease (*). Annu Rev Immunol 2009;27:621-68.
35. Muruve DA, Petrilli V, Zaiss AK, White LR, Clark SA, Ross PJ, et al. The inflammasome recognizes cytosolic microbial and host DNA and triggers an innate immune response. Nature 2008;452:103-7.
36. Zhou R, Tardivel A, Thorens B, Choi I, Tschopp J. Thioredoxin-interacting protein links oxidative stress to inflammasome activation. Nat Immunol 2010;11:136-40.
37. Martinon F, Petrilli V, Mayor A, Tardivel A, Tschopp J. Gout-associated uric acid crystals activate the NALP3 inflammasome. Nature

2006;440:237-41.

38. Mariathasan S, Weiss DS, Newton K, McBride J, O'Rourke K, Roose-Girma M, et al. Cryopyrin activates the inflammasome in response to toxins and ATP. Nature 2006;440:228-32.

39. Yamasaki K, Muto J, Taylor KR, Cogen AL, Audish D, Bertin J, et al. NLRP3/cryopyrin is necessary for interleukin-1beta (IL-1beta) release in response to hyaluronan, an endogenous trigger of inflammation in response to injury. J Biol Chem 2009;284:12762-71.

40. Li H, Ambade A, Re F. Cutting edge: Necrosis activates the NLRP3 inflammasome. J Immunol 2009;183:1528-32.

41. Goncalves RG, Gabrich L, Rosario A, Jr., Takiya CM, Ferreira ML, Chiarini LB, et al. The role of purinergic P2X7 receptors in the inflammation and fibrosis of unilateral ureteral obstruction in mice. Kidney Int 2006;70:1599-606.

42. DeWolf SE, Shigeoka AA, Scheinok A, Kasimsetty SG, Welch AK, McKay DB. Expression of TLR2, NOD1, and NOD2 and the NLRP3 Inflammasome in Renal Tubular Epithelial Cells of Male versus Female Mice. Nephron 2017;137:68-76.

43. Yu JW, Lee MS. Mitochondria and the NLRP3 inflammasome: physiological and pathological relevance. Arch Pharm Res 2016;39:1503-18.

44. Zhou R, Yazdi AS, Menu P, Tschopp J. A role for mitochondria in NLRP3 inflammasome activation. Nature 2011;469:221-5.

45. Liang H, Ward WF. PGC-1alpha: a key regulator of energy metabolism. Adv Physiol Educ 2006;30:145-51.

46. Soriano FX, Liesa M, Bach D, Chan DC, Palacin M, Zorzano A. Evidence for a mitochondrial regulatory pathway defined by peroxisome proliferator-activated receptor-gamma coactivator-1 alpha, estrogen-related receptor-alpha, and mitofusin 2. Diabetes 2006;55:1783-91.

47. Vainshtein A, Tryon LD, Pauly M, Hood DA. Role of PGC-1alpha during acute exercise-induced autophagy and mitophagy in skeletal muscle. Am J Physiol Cell Physiol 2015;308:C710-9.
48. Tran M, Tam D, Bardia A, Bhasin M, Rowe GC, Kher A, et al. PGC-1alpha promotes recovery after acute kidney injury during systemic inflammation in mice. J Clin Invest 2011;121:4003-14.
49. Li SY, Susztak K. The Role of Peroxisome Proliferator-Activated Receptor gamma Coactivator 1alpha (PGC-1alpha) in Kidney Disease. Semin Nephrol 2018;38:121-6.
50. Zhang L, Liu J, Zhou F, Wang W, Chen N. PGC-1alpha ameliorates kidney fibrosis in mice with diabetic kidney disease through an antioxidative mechanism. Mol Med Rep 2018;17:4490-8.
51. Portilla D, Dai G, McClure T, Bates L, Kurten R, Megyesi J, et al. Alterations of PPARalpha and its coactivator PGC-1 in cisplatin-induced acute renal failure. Kidney Int 2002;62:1208-18.
52. Kang HM, Ahn SH, Choi P, Ko YA, Han SH, Chinga F, et al. Defective fatty acid oxidation in renal tubular epithelial cells has a key role in kidney fibrosis development. Nat Med 2015;21:37-46.
53. Diao L, Marshall AH, Dai X, Bogdanovic E, Abdullahi A, Amini-Nik S, et al. Burn plus lipopolysaccharide augments endoplasmic reticulum stress and NLRP3 inflammasome activation and reduces PGC-1alpha in liver. Shock 2014;41:138-44.
54. Lv J, Bhatia M, Wang X. Roles of Mitochondrial DNA in Energy Metabolism. Adv Exp Med Biol 2017;1038:71-83.
55. Decleves AE, Sharma K. Novel targets of antifibrotic and anti-inflammatory treatment in CKD. Nat Rev Nephrol 2014;10:257-67.
56. Rasbach KA, Schnellmann RG. Signaling of mitochondrial biogenesis following oxidant injury. J Biol Chem 2007;282:2355-62.
57. Wu Z, Puigserver P, Andersson U, Zhang C, Adelmant G, Mootha V, et

al. Mechanisms controlling mitochondrial biogenesis and respiration through the thermogenic coactivator PGC-1. Cell 1999;98:115-24.

58. Handschin C, Spiegelman BM. Peroxisome proliferator-activated receptor gamma coactivator 1 coactivators, energy homeostasis, and metabolism. Endocr Rev 2006;27:728-35.

59. Lehman JJ, Barger PM, Kovacs A, Saffitz JE, Medeiros DM, Kelly DP. Peroxisome proliferator-activated receptor gamma coactivator-1 promotes cardiac mitochondrial biogenesis. J Clin Invest 2000;106:847-56.

60. Rasbach KA, Schnellmann RG. PGC-1alpha over-expression promotes recovery from mitochondrial dysfunction and cell injury. Biochem Biophys Res Commun 2007;355:734-9.

61. Puigserver P, Wu Z, Park CW, Graves R, Wright M, Spiegelman BM. A cold-inducible coactivator of nuclear receptors linked to adaptive thermogenesis. Cell 1998;92:829-39.

62. Weinberg JM. Mitochondrial biogenesis in kidney disease. J Am Soc Nephrol 2011;22:431-6.

63. Kang Y, Zhang H, Zhao Y, Wang Y, Wang W, He Y, et al. Telomere Dysfunction Disturbs Macrophage Mitochondrial Metabolism and the NLRP3 Inflammasome through the PGC-1alpha/TNFAIP3 Axis. Cell Rep 2018;22:3493-506.

64. Yu X, Mao W, Zhai Y, Tong C, Liu M, Ma L, et al. Anti-tumor activity of metformin: from metabolic and epigenetic perspectives. Oncotarget 2017;8:5619-28.

65. El-Mir MY, Nogueira V, Fontaine E, Averet N, Rigoulet M, Leverve X. Dimethylbiguanide inhibits cell respiration via an indirect effect targeted on the respiratory chain complex I. J Biol Chem 2000;275:223-8.

ABSTRACT (IN KOREAN)

PGC-1α의 미토콘드리아 기능 및 NLRP3 inflammasome 활성화 조절을 통한 신장 세뇨관-간질 섬유화 억제 효과

< 지도교수 한 승 혁 >

연세대학교 대학원 의학과

지 종 현

배경: NOD-like receptor, pyrin domain containing protein 3 (NLRP3)는 신장 질환에서 염증 반응, 세포사멸, 신섬유화에 기여하는 것으로 알려져 있다. NLRP3 인플라마좀 (inflammasome)은 미토콘드리아 손상에 의해 활성화 되나, 미토콘드리아의 활성 조절에 필수적인 peroxisomal proliferator-ɣ coactivator-1α (PGC-1α)가 NLRP3 인플라마좀 활성화에 기여하는 역할에 대해서는 밝혀진 바 없다.

목적: 본 연구에서는 신섬유화 과정에서 PGC-1α가 미토콘드리아의 구조 및 활성 조절을 통하여 NLRP3 인플라마좀의 활성화에 미치는 영향을 알아보고자 하였다.

방법: C57BL/6 쥐로부터 일차 세포 배양을 통해 얻은 신세뇨관 상피세포에 48시간동안 TGF-β1을 투여하여 신섬유화를 유발시킨 후 PGC-1α를 간접적 혹은 직접적으로 과발현, siRNA를 처리하여 그 발현을 저하시켜, NLRP3 인플라마좀, 미토콘드리아 형태 및 활성, 신섬유화 및 세포 사멸 관련 인자들의 변화를 확인하였다. 동물실험으로는 C57BL/6 쥐에 아데닌 (adenine) 사료를 4주간 먹인 모델과 일측성 요관 폐쇄를 시행한 신장 질환 모델에서 PGC-1α

활성화 약물을 투약 후, NLRP3 인플라마좀, 미토콘드리아 형태 및 활성, 신섬유화 및 세포 사멸 관련 인자들의 변화를 확인하였다.

결과: TGF-β1을 투여한 신세뇨관 상피 세포에서 PGC-1α 및 미토콘드리아의 형태 관련 인자들의 발현이 감소하고, NLRP3 인플라마좀과 섬유화, 세포 사멸에 관련한 인자들의 발현은 증가하는 것을 확인하였다. 반면, PGC-1α 간접 혹은 직접적인 과발현 시 미토콘드리아의 손상은 회복되고 활성산소종은 감소하며, tumor necrosis factor α induced protein 3 (TNFAIP3)의 발현이 증가하고, NLRP3 인플라마좀 및 섬유화, 세포 사멸 인자들의 발현은 감소하는 것을 확인하였다. siRNA로 PGC-1α의 발현을 저하시킨 경우, 그 반대의 결과들을 관찰하였다. 아데닌 사료 투여 및 일측성 요관 폐쇄 동물 모델에서도 PGC-1α 활성화 약물 투약 시 미토콘드리아의 손상은 회복되었고, 산화 스트레스의 감소 및 TNFAIP3 발현의 증가를 관찰 할 수 있었으며, NLRP3 인플라마좀 및 섬유화, 세포 사멸 인자들의 발현이 감소하는 것을 확인하였다.

결론: 이상의 결과를 종합하여 볼 때, 신섬유화 과정에서 PGC-1α에 의한 미토콘드리아 기능의 회복 및 활성산소종의 억제, TNFAIP3 발현의 증가는 NLRP3 인플라마좀의 활성을 억제하여 신손상을 완화시키는 것으로 생각된다.

핵심되는 말: NLRP3, PGC-1α, 미토콘드리아, 신섬유화